Assessment of Density Functional Theory for Model S_N2 Reactions: $CH_3X + F^-$ (X = F, Cl, CN, OH, SH, NH_2, PH_2)

Jason M. Gonzales, R. Sidney Cox III, Shawn T. Brown, Wesley D. Allen, and Henry F. Schaefer III*

Center for Computational Quantum Chemistry, University of Georgia, Athens, Georgia 30602-2525

Received: July 26, 2001; In Final Form: October 8, 2001

The B3LYP, BLYP, and BP86 variants of density functional theory, in conjunction with double and triple ζ basis sets, have been examined for S_N2 reactions of the type $CH_3X + F^- \rightarrow CH_3F + X^-$ (X = F, Cl, CN, OH, SH, NH_2, and PH_2), using the CCSD(T) method in combination with the TZ2Pf+dif and aug-cc-pVTZ basis sets as a reference for comparison, along with experimental calibrations. The functionals perform modestly well, with some preference for B3LYP, in describing the structures of the stationary points, nonetheless exhibiting bond distance deviations as large as 0.24 Å and bond angle deviations as large as 39°. Regarding the energetics, the three functionals perform best for ion−molecule complexation energies ($E^w_{X,Y}$), on average deviating by 1.3 kcal mol^{-1}. However, the pure functionals are not able to characterize the reaction energies ($E^0_{X,Y}$) and particularly the net activation barriers ($E^b_{X,Y}$) with the same accuracy, with underestimations as large as 11.0 kcal mol^{-1} for S_N2 barriers. The hybrid B3LYP functional significantly outperforms the pure functionals for these same energetic quantities, better approximating the coupled cluster reference by over 4 kcal mol^{-1}. Still however, B3LYP is only marginally satisfactory. In fact, all of the functionals give S_N2 transition states which are anomalously too low in energy, revealing the need for reconstructions and reparametrizations for accurate treatments of these pervasive reactions. Comparison of CCSD(T)/TZ2Pf+dif with CCSD(T)/aug-cc-pVTZ shows the need to use high level extrapolation schemes to describe the energetics of these types of reactions to within one kcal mol^{-1}.

I. Introduction

Bimolecular nucleophilic substitution (S_N2) reactions at carbon centers are among the most intensely studied of all chemical reactions. The class of reactions, as exemplified by eq 1

$$Y^- + CH_2RX \rightarrow [Y - CH_2R - X]^{-\ddagger} \rightarrow YCH_2R + X^- \quad (1)$$

has been investigated by an exceptional array of kinetic experiments,[1−10] ab initio quantum and semiclassical dynamical methods and trajectory simulations,[11−18] statistical mechanical studies,[19−26] ab initio and density functional structural analyses,[27−39] and electron-transfer studies,[40−45] meriting recent articles in high-profile journals.[46,47] Since the early 1970s, much work has focused on ion−molecule reaction dynamics in the gas phase in order to more clearly expose intrinsic versus solvent effects in solution. As a consequence, S_N2 reactions have become models for achieving both qualitative and quantitative understandings of ion−molecule reactions in general.

The pioneering experimental and theoretical[46,48,49] work of the 1970s showed that the general reaction-energy profile for gas-phase S_N2 displacements exhibits a double well potential separated by a central barrier, as depicted in Figure 1 for the reaction of F^- and CH_3X. Several basic questions regarding the microscopic structure and dynamics displayed by these surfaces have attracted a continuing flow of research activity. First, there has been confusion over the precise electronic structure factors which determine the height of the central barrier. For example, theory[46,49] has revealed that the stabilization of the S_N2 transition state by α substitution can be mostly due to inherent electrostatics rather than resonance delocalization, as in the case of identity exchange in the chloroacetonitrile system, whose reaction rate has been studied extensively by Wladkowski et al.[50] and Viggiano et al.[51] Second, the collisional association of Y^- with CH_2RX entails the transfer of relative translational energy to vibrational and/or rotational motion of the $[Y-CH_3X]^-$ ion−molecule intermediate, the key issue being whether the system is trapped long enough in this prereaction complex to achieve the energy randomization assumed in statistical (RRKM or μVTST) theories. For several simple methyl halide systems, there is theoretical evidence of limited energy redistribution and direct S_N2 displacement without prior trapping, i.e., nonstatistical behavior.[48,52−56] Among seven S_N2 reactions targeted in one set of experimental studies,[51,57−60] those involving methyl halides showed reaction rates which depended on the particular type of energy present, whereas the reactivity

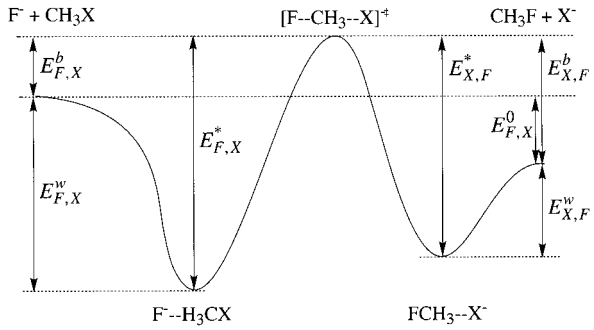

Figure 1. Energy diagram for a prototypical gas-phase S_N2 reaction. Note the double well with two minima corresponding to ion-molecule complexes.

10.1021/jp012892a CCC: $20.00 © 2001 American Chemical Society
Published on Web 11/22/2001

TABLE 1: Heats of Formation ($\Delta_f H_0^\circ$; kcal mol^{-1}) Utilized in This Paper

	$\Delta_f H_0^\circ$	ref
F^- [a]	−59.9	65
Cl^- [a]	−58.8	65
CN^- [b]	18.7	66
OH^- [b]	−31.3	66
SH^- [b]	−18.0	66
NH_2^- [b]	29.1	66
PH_2^- [b]	8.2	66
CH_3F [a]	−57.0	63
CH_3Cl [a]	−18.1	65
CH_3CN [b]	19.9	66
CH_3OH [b,c]	−46.1	66
CH_3SH [b,c]	−3.2	66
CH_3NH_2 [b,c]	−3.4	66
CH_3PH_2 [b,c]	−2.5	64

[a] Experimental $\Delta_f H_0^\circ$ values. [b] These values utilized experimental $\Delta_f H_{298}^\circ$, and corrected to $\Delta_f H_0^\circ$. Unscaled MP2/TZ2Pf+dif harmonic frequencies were used for the vibrational correction. [c] The barriers to internal rotation of these molecules were computed (B3LYP/TZ2Pf+dif) to be 1.35 (CH_3OH), 5.01 (CH_3SH), 2.35 (CH_3NH_2) and 2.00 kcal mol^{-1} (CH_3PH_2). The effect on the heats of formation of assuming a hindered rotor, rather than a harmonic oscillator, and using the analysis of Pitzer and Gwinn[116] was under 0.1 kcal mol^{-1} in each case.

in other systems depended only on total available energy. Third, there is considerable interest in whether the general displacement process, the surmounting of the central barrier for S_N2 reactions, can be enhanced by selective vibrational excitation of AX.[48] Finally, recrossing the central barrier in model systems such as $CH_3Cl + Cl^-$ has been shown via classical trajectory simulations to reduce the reaction rate to only 10%−30% of that predicted by transition state theories,[48,61] raising the specter of frequent deficiencies of such theories for S_N2 reactions.

Recent advances in density functional theory (DFT) have elevated this methodology as a powerful tool for electronic structure problems, particulary for large systems which are poorly described by uncorrelated Hartree−Fock wave functions. In a 1995 article, Ziegler[62] expressed the expectation that "DFT will become as indispensable a research tool in chemistry as any major spectroscopic technique". Of course, the continuing fulfillment of this expectation depends on careful calibration studies to establish the reliability of density functional theory and to indicate necessary enhancements.

Toward this end, we perform in this research systematic calibration studies of three of the best and most widely employed DFT methods (in particular the B3LYP, BLYP, and BP86 functionals) on the stationary points of the prototypical S_N2 reactions

$$F^- + CH_3X \rightarrow FCH_3 + X^- \qquad (2)$$

with X being F, Cl, CN, OH, SH, NH_2, and PH_2. The resulting predictions are compared to those of coupled cluster singles and doubles theory augmented by a perturbative contribution from connected triple excitations [CCSD(T)]. Thermochemical comparisons are also made with the limited available experimental data on reaction enthalpies, derived from the heats of formation collected in Table 1.[63−66] The key energetic quantities of eq 2, as depicted in Figure 1, are labeled as follows: $E_{F,X}^w$ ($E_{X,F}^w$) is the well depth for the entering (leaving) ion−molecule complexes; $E_{F,X}^*$ ($E_{X,F}^*$) is the intrinsic activation barrier for the forward (reverse) reaction; $E_{F,X}^b$ ($E_{X,F}^b$) is the net activation barrier for the forward (reverse) reaction, and $E_{F,X}^0$ is the forward reaction energy.

$$E_{F,X}^w = E(F^-\cdot CH_3X) - E(CH_3X) - E(F^-) \qquad (3)$$

$$E_{F,X}^b = E[(F - CH_3 - X)^{-\ddagger}] - E(CH_3X) - E(F^-) \qquad (4)$$

$$E_{F,X}^* = E[(F - CH_3 - X)^{-\ddagger}] - E(F^-\cdot CH_3X) \qquad (5)$$

$$E_{X,F}^w = E(FCH_3\cdot X^-) - E(CH_3F) - E(X^-) \qquad (6)$$

$$E_{X,F}^b = E[(F - CH_3 - X)^{-\ddagger}] - E(CH_3F) - E(X^-) \qquad (7)$$

$$E_{X,F}^* = E[(F - CH_3 - X)^{-\ddagger}] - E(FCH_3\cdot X^-) \qquad (8)$$

$$E_{F,X}^0 = E(CH_3F) + E(X^-) - E(CH_3X) - E(F^-) \qquad (9)$$

Some of the earliest work employing density functional theory for S_N2 types of reactions was performed by Bickelhaupt, Baerands, Nibbering, and Ziegler.[28] They utilized the X_α functional in conjuction with a DZP basis set to look at elimination and substitution reactions between F^- and CH_3CH_2F. Their work was subsequently analyzed in 1995 by Gronert, Merrill, and Kass,[32] who calculated large deviations between the Bickelhaupt results and their own G2+ method. The deviations included structural differences of over 0.7 Å for some bond distances. Gronert et al. also found the density functionals to underestimate the complexation energy by almost 6 kcal mol^{-1}.

Subsequent work of this type was executed by Deng, Branchadell, and Ziegler,[29] who compared results from the local density approximation (LDA) and nonlocal Becke-Perdew functionals (termed NL-SCF) with conventional predictions for the CH_3X/X^- halide identity exchange reactions. Although some of the results are encouraging, some serious problems with the DFT methods were discovered, viz., the central S_N2 barriers were generally too small. For the CH_3F/F^- system, the better DFT method (NL-SCF) gave a complexation energy of 19.9 kcal mol^{-1} and an intrinsic barrier of 6.8 kcal mol^{-1}, whereas a definitive ab initio investigation[31] has pinpointed these quantities at 13.6 and 12.8 kcal mol^{-1}, respectively.

Glukhovtsev, Bach, Pross, and Radom[33] performed an analysis of the B3LYP functional, in conjunction with the 6−31-(d) and 6-311+G(3df,2p) basis sets for the $Cl^- + CH_3Cl$ and $Cl^- + CH_3Br$ reactions, comparing the DFT variant to the MP2, MP4 and G2 methods. They determined that "reasonable values of the complexation energy" were obtained. However, they also found that the net and intrinsic activation barriers were "significantly underestimated when compared to G2(+) or experimental results". Nevertheless, the work was limited to the B3LYP functional, and the basis sets of Pople and co-workers.[67,68]

Finally, in a very recent paper, Parthiban, de Oliveira and Martin[39] performed very high level extrapolations on reactions of the type $CH_3Y + X^-$, X = F, Cl, Br. They utilized B3LYP/cc-pVTZ+1 (inclusion of a tight *d* function in the basis set) reference geometries in calculating very high level extrapolated energetics. They claim that B3LYP/cc-pvTZ+1 provides "geometries for stable molecules ... within a few thousandths of an Å from experiment".

It is the goal of this work to systematically look at some of these reactions to compare currently employed density functional methods to highly correlated ab initio methods. The limited previous work shows some instances with large deviations, both structural and energetic, between density functional and ab initio methods. In light of the burgeoning use of DFT methods, these discrepancies are serious and demand thorough research.

II. Computational Methods

The density functional methods employed in this paper are based on the B3LYP, BLYP and BP86 functionals. The B3LYP functional is a combination of the hybrid three-parameter Becke exchange functional[69] and the Lee−Yang−Parr correlation functional (LYP).[70] The BLYP functional is a pure DFT method using the exchange functional of Becke (B)[71] with the Lee−Yang−Parr correlation functional (LYP). The BP86 functional is also a pure DFT method using the exchange functional of Becke (B)[71] and the correlation functional of Perdew (P86).[72]

In addition to density functional predictions, results are reported here from coupled cluster theory, namely the coupled cluster singles and doubles method, including a perturbative contribution for connected triple excitations, CCSD(T).[73−76] Owing to a dearth of experimental information, the coupled cluster values provide critical, highly correlated ab initio benchmarks for the DFT assessment, but they will not be overly analyzed here. They will be detailed in a future publication[114] discussing the same reactions.

Three distinct Gaussian basis sets were used for most of this study. They are referred to as DZP+dif, TZ2P+dif and TZ2Pf+dif and are detailed as follows. The DZP+dif basis set consists of the double-ζ *sp* contractions of Dunning and Huzinaga[77,78] for hydrogen and first-row atoms, and the double-ζ *sp* contractions of Dunning[79] for second-row atoms, augmented with one set of polarization functions and a set of diffuse functions (a diffuse *s* for hydrogen and a diffuse *s* and *p* for heavy atoms). The polarization exponents for this set are as follows: $\alpha_p(H) = 0.75$, $\alpha_d(C) = 0.75$, $\alpha_d(N) = 0.8$, $\alpha_d(O) = 0.85$, $\alpha_d(F) = 1.0$, $\alpha_d(P) = 0.6$, $\alpha_d(S) = 0.7$, and $\alpha_d(Cl) = 0.75$. It should be noted that a typographical error in the listing of the DZ basis set of sulfur in ref 79 was remedied here, namely $\alpha_s = 0.4246$ was corrected to 0.4264.

The diffuse functions added were constructed to be even tempered, following the guidelines of Lee and Schaefer.[80] That is, the *s* or *p* type diffuse function exponent, $\alpha_{diffuse}$, for a given atom was determined by

$$\alpha_{diffuse} = \frac{1}{2}\left(\frac{\alpha_1}{\alpha_2} + \frac{\alpha_2}{\alpha_3}\right)\alpha_1 \qquad (10)$$

where α_1, α_2 and α_3 are the first, second and third smallest Gaussian orbital exponents, in order, of the *s* or *p* type primitive functions of the atom.

The TZ2P+dif basis set consists of the triple-ζ *sp* contractions of Dunning[81] for hydrogen and first-row atoms and the (12*s*9*p*/6*s*5*p*) triple-ζ *sp* contraction of McLean and Chandler[82] for second-row atoms, augmented with two sets of polarization functions and a set of diffuse functions (the same functions as in DZP+dif). The polarization exponents are as follows: $\alpha_p(H) = 0.375, 1.5$; $\alpha_d(C) = 0.375, 1.5$; $\alpha_d(N) = 0.4, 1.6$; $\alpha_d(O) = 0.425, 1.7$; $\alpha_d(F) = 0.5, 2.0$; $\alpha_d(P) = 0.3, 1.2$; $\alpha_d(S) = 0.35, 1.4$; and $\alpha_d(Cl) = 0.375, 1.5$.

The TZ2Pf+dif basis set is constructed by adding one final set of higher angular momentum functions to TZ2P+dif. This is a set of *d* functions on hydrogens and a set of *f* functions on the heavy atoms. The exponents are as follows: $\alpha_d(H) = 1.0$, $\alpha_f(C) = 0.8$, $\alpha_f(N) = 1.0$, $\alpha_f(O) = 1.4$, $\alpha_f(F) = 1.85$, $\alpha_f(P) = 0.45$, $\alpha_f(S) = 0.55$, and $\alpha_f(Cl) = 0.7$.

Final single-point CCSD(T) energies were computed with the aug-cc-pVTZ basis set of Dunning, Kendall, and Harrison.[83,84] For these calculations, only valence electrons were correlated. These computations were primarily done to assess basis set convergence. In all cases, the aug-cc-pVTZ calculations supersede the TZ2Pf+dif results, i.e., the CCSD(T)/aug-cc-pVTZ results are our definitive computational results. A future publication[115] will include energetic extrapolations with basis sets of at least 5ζ quality.

The final contractions for the three primary basis sets are as follows. For DZP+dif: hydrogen (5*s*1*p*/3*s*1*p*), first-row atoms (10*s*6*p*1*d*/5*s*3*p*1*d*), and second-row atoms (12*s*8*p*1*d*/7*s*5*p*1*d*). For TZ2P+dif: hydrogen (6*s*2*p*/4*s*2*p*), first-row atoms (11*s*7*p*2*d*/6*s*4*p*2*d*), and second-row atoms (13*s*10*p*2*d*/7*s*6*p*2*d*). Finally, for TZ2Pf+dif: hydrogen (6*s*2*p*1*d*/4*s*2*p*1*d*), first-row atoms (11*s*7*p*2*d*1*f*/6*s*4*p*2*d*1*f*,) and second-row atoms (13*s*10*p*2*d*1*f*/7*s*6*p*2*d*1*f*). All basis sets involve pure angular momentum *d* and *f* manifolds. The use of these basis sets for density functional calculations has been previously reported,[85−88] with good agreement with experiment. The effect of basis set superposition error (BSSE) on complexation energies was analyzed using the counterpoise procedure,[89,90] and found to generally be less than 0.5 kcal mol^{-1} for the aug-cc-pVTZ calculations.

All density functional geometry optimizations and frequency calculations utilized analytic first and second derivatives, respectively. Coupled cluster optimizations were also performed with analytic first derivatives. Optimizations were carried out in internal coordinates. All Cartesian forces at the optimized geometries were below 2.5×10^{-5} hartrees/bohr for the DFT methods and 1.0×10^{-6} hartree/bohr for the coupled cluster methods. Vibrational frequency evaluations were performed at all density functional optimized structures to ensure local minimum or transition state (first-order saddle point) character and to determine the zero-point vibrational corrections. No core electrons or virtual orbitals were frozen during the coupled cluster optimizations. All density functional computations were performed using the GAUSSIAN 94[91] computational package, whereas coupled cluster calculations utilized the ACESII[92] package. Due to the abundance of data (over 350 DFT optimizations and frequency calculations, and over 100 CCSD(T) optimizations), not all calculated values are included in this paper, but complete information can be obtained in the Supporting Information.

III. Results

Because the number of structures with attendant energetics presented in this paper is large, the reactions are discussed in individual subsections. After all of the data have been presented, the results will be summarized collectively. Due to space considerations only the structural information from the calculations with the largest basis set, i.e., TZ2Pf+dif, is shown. All structural quantities, all vibrational frequencies, and statistics for individual reactions are included in the Supporting Information. There is only limited structural deviation among the functionals as the basis set is varied, as shown by the statistics in Table 2. Note the significant improvement in convergence when the basis is changed from TZ2P+dif to TZ2Pf+dif, compared to the change from DZP+dif to TZ2P+dif. As expected, the DFT basis set dependence is generally substantially smaller than that for CCSD(T). Finally, the deviations in bond distances are similar when considering heavy atom−hydrogen bonds vs heavy atom−heavy atom bonds.

Two of the five stationary points of the S_N2 reaction shown in Figure 1 are ion−molecule complexes. In general, several conceivable geometries are possible for this type of structure. Glukhovtsev, Pross, and Radom[30,93] discuss several of the possibilities in their previous work on corresponding S_N2 reactions. We began our study by considering linear backside attack, but observed minimum structures of this type for only

TABLE 2: Average Absolute Deviation in Geometric Parameters as Basis Set Size Is Increased[a]

	DZP+dif to TZ2P+dif				TZ2P+dif to TZ2Pf+dif			
	B3LYP	BLYP	BP86	CCSD(T)	B3LYP	BLYP	BP86	CCSD(T)
r	0.010	0.011	0.009	0.013	0.003	0.003	0.003	0.007
r_{X-H}[b]	0.010	0.011	0.009	0.011	0.002	0.002	0.002	0.004
r_{X-Y}	0.010	0.011	0.010	0.016	0.005	0.006	0.006	0.012
θ	0.688	0.691	0.682	1.317	0.224	0.265	0.268	0.338
τ	1.008	1.629	1.040	3.242[c]	0.219	0.249	0.279	0.103

[a] Bond distance deviations are in Å whereas bond and torsional angle deviations are in degrees. [b] X−H signifies heavy atom−hydrogen bond distance, whereas X−Y signifies heavy atom−heavy atom bond distance. [c] If two outlying torsional deviations are removed, this average deviation lowers to 1.480°.

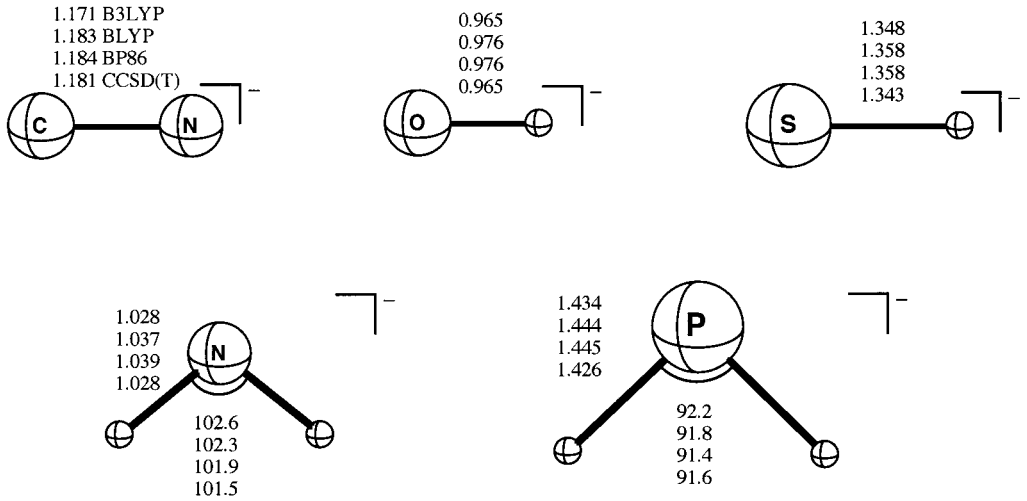

Figure 2. Geometries of the leaving group anions. All bond distances are in Å and bond angles in degrees. All reported values utilize the TZ2Pf+dif basis set.

two of the seven reactions. The potential energy surfaces were scanned at many possible structures, using the smaller DZP+dif basis set, to ensure that no relevant ion−molecule complexes were present other than those reported here. Some previous work has assumed linear backside attack, and computed corresponding stationary points, but not tested for stability. Analytic second derivatives of all structures were computed here with the three density functionals to ensure true minimum character of our ion−molecule complexes, and first-order saddle-point character of our transition states.

A. Leaving Group Ions and Neutral Substrates. We begin our data presentation by considering the structures of the leaving group anions and neutral substrates. For the diatomic and triatomic leaving groups (shown in Figure 2), the general trend has the B3LYP functional in closest agreement with our reference method CCSD(T) for bond distances, whereas BP86 is closest for bond angles. The average absolute deviations with respect to the coupled cluster reference are 0.004, 0.011, and 0.012 Å for bond distances and 0.7, 0.5 and 0.3° for bond angles for B3LYP, BLYP, and BP86, respectively. The largest deviation in bond distance is 0.019 Å (BP86 r_{P-H}), and in bond angle 1.1° (B3LYP θ_{H-N-H}).

Figure 3 shows the structural information for the seven neutral substrates. CH_3F, CH_3Cl, and CH_3CN all have C_{3v} symmetry, with all methyl hydrogens equivalent, whereas CH_3OH, CH_3SH, CH_3NH_2, and CH_3PH_2 all have C_s symmetry. Here, it is important to make a distinction between two types of bond distances, heavy atom−hydrogen and heavy atom−heavy atom. We report values and statistics for both quantities; however, the heavy atom−hydrogen bond distance deviations among methods are consistently smaller for a given basis set, by almost one order of magnitude.

The seven neutral substrates are all tightly bound, and we expect density functional theory to describe their structures in good agreement with CCSD(T). This is indeed what is observed. Vis-à-vis the CCSD(T) benchmark, B3LYP systematically outperforms the pure functionals for bond distances (average deviations of 0.005 Å vs 0.012−0.013 Å), although the DFT angle predictions are virtually indistinguishable in quality. In general the functionals tend to slightly overestimate the bond distances and angles. The largest deviation in a heavy-atom bond is 0.033 Å (BLYP r_{C-Cl}), and in a heavy atom-hydrogen bond 0.020 Å (BP86 r_{P-H}). For bond angles the largest deviation is 1.4° (B3LYP θ_{H-N-C} CH_3NH_2), whereas for torsional angles the largest deviation is 1.5° (B3LYP $\tau_{H'CNH}$ CH_3NH_2). In brief, for both the leaving groups and neutral substrates the DFT methods give structural predictions of expected (reasonably good) accuracy.

B. $CH_3F + F^- \rightarrow CH_3F + F^-$. The identity S_N2 reaction with F^- as both a nucleophile and a leaving group is the most studied of the S_N2 reactions theoretically.[27,29−31,94−99] A definitive work was published by Wladkowski, Allen, and Brauman in 1994.[31] Their work includes optimizations of all structures with a QZ2P+dif basis set at the CCSD level. They further expand on their optimizations by employing the focal-point method[100−104] to extrapolate toward the nonrelativistic ab initio limit with basis sets including over 430 functions. In a more recent paper, Parthiban, de Oliveira and Martin[39] utilized the W1, W1′, and W2h extrapolation schemes, with basis sets of up to aug-cc-pV5Z quality, to characterize the energetics associated with this reaction, based on B3LYP/cc-pVTZ+1 structures. As seen below, the use of such DFT reference structures may be questioned, but the concomitant effects on the energetics may not be very substantial.

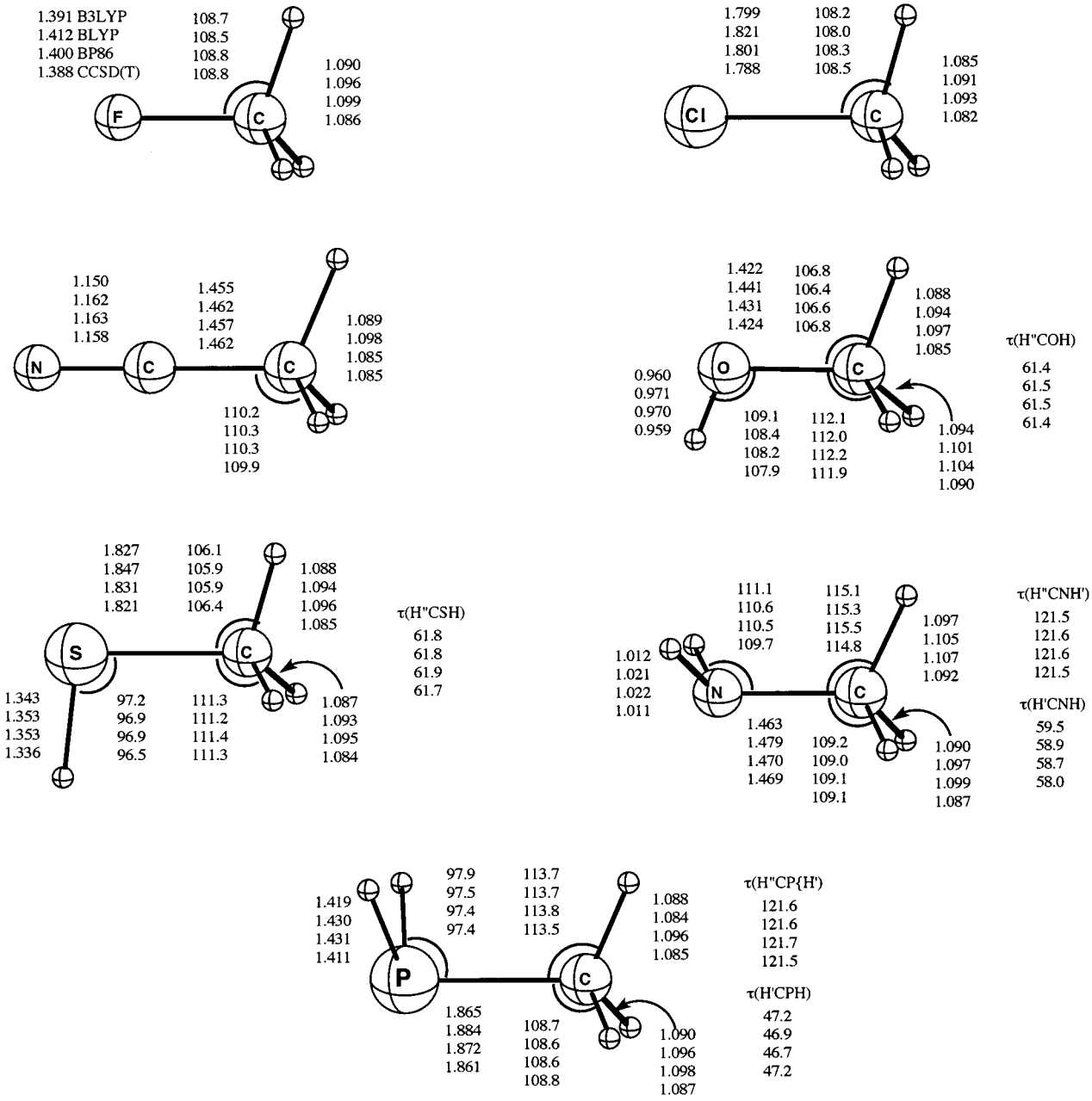

Figure 3. Geometries of the neutral substrate reactants. All bond distances are in Å, bond and torsional angles in degrees. CH_3F, CH_3Cl, and CH_3CN are in C_{3v} symmetry, while the others are in C_s. The heavy atoms and the unique methyl hydrogen are in the plane of the paper. The notation of this and all subsequent figures has H as a leaving group hydrogen (e.g., an NH_2 hydrogen), H′ as the unique methyl hydrogen, and H″ as the symmetry-equivalent methyl hydrogens.

The structures for the $CH_3F + F^-$ reaction are detailed in Figure 4. Because this is an identity exchange reaction, there is only one distinct ion−molecule complex. The $F^-{\cdot}H_3CF$ adduct is primarily electrostatic in character,[31,94] exhibiting a C_{3v} structure with optimal ion−dipole alignment. The intermolecular F^-−C distance is found to be quite large, over 2.5 Å. The CCSD(T)/TZ2Pf+dif computed result is 0.023 Å smaller than the CCSD/QZ2P+dif distance of 2.598 Å calculated by Wladkowski et al.[31] Among the DFT predictions for the intermolecular separation, the B3LYP and BLYP F^-−C distances are quite close (within 0.015 Å) to the TZ2Pf+dif CCSD(T) reference, whereas the BP86 distance is substantially (0.038 Å) shorter. The C−F distance of the substrate is elongated by about 0.05 Å compared to isolated CH_3F (there is minimal change in the bond angle). Here, both BLYP and BP86 show suprisingly large variances with CCSD(T), overestimating this C−F length by 0.050 Å and 0.034 Å, respectively.

For the S_N2 transition state, in D_{3h} symmetry, all DFT methods overestimate the critical F−C distance, by 0.027−0.065 Å. For r_{C-H} B3LYP is within 0.002 Å of the reference, whereas BP86 deviates by 0.012 Å. For r_{F-C} our CCSD(T) reference is in precise agreement with the Wladkowski value of 1.826 Å.

Finally, the energetic quantities associated with this reaction are considered, as listed in Table 3. In general, $E^*_{X,Y}$ will not be discussed, because it is merely the sum of $E^b_{F,F}$ and $E^w_{F,F}$, but we list it for convenience. For the complexation energy, $E^w_{F,F}$, the functionals are never more than 0.75 kcal mol^{-1} removed from the CCSD(T)/TZ2Pf standard of −13.28 kcal mol^{-1}. In all cases, the agreement between TZ2Pf+dif and aug-cc-pVTZ CCSD(T) is within 0.75 kcal mol^{-1}. The CCSD(T) values compare favorably with the Wladkowski et al.[31] value of −13.58 kcal mol^{-1} and the Parthiban et al.[39] value of −13.38 kcal mol^{-1}.

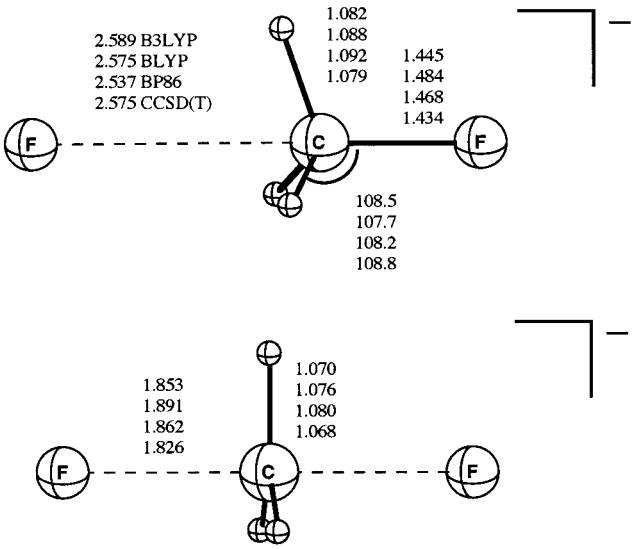

Figure 4. Geometries of the ion−molecule complex and transition state for the reaction $CH_3F + F^-$ using the TZ2Pf+dif basis set. All bond distances are in Å and bond angles in degrees. The ion−molecule complex is in C_{3v} symmetry while the transition state is in D_{3h} symmetry.

TABLE 3: Energetics (kcal mol^{-1}) of the $CH_3F + F^- \rightarrow CH_3F + F^-$ Reaction[a]

	$E^b_{F,F}$	$E^w_{F,F}$	$E^*_{F,F}$
	DZP + dif		
B3LYP	−2.09	−13.02	10.93
BLYP	−5.90	−13.06	7.16
BP86	−5.27	−12.88	7.61
CCSD(T)	1.16	−13.42	14.58
	TZ2P + dif		
B3LYP	−3.72	−13.08	9.36
BLYP	−7.44	−13.19	5.75
BP86	−6.89	−13.04	6.15
CCSD(T)	−2.15	−13.65	11.51
	TZ2Pf + dif		
B3LYP	−2.81(−3.05)	−12.87(−12.74)	10.06(9.69)
BLYP	−6.62(−6.97)	−12.93(−12.91)	6.31(5.94)
BP86	−6.05(−6.39)	−12.79(−12.81)	6.74(6.42)
CCSD(T)	−0.38(−0.53)	−13.49(−13.28)	13.11(12.75)
aug-cc-pVTZ[b]	(−1.25)	(−13.95)	(12.69)

[a] The numbers in parentheses are zero-point corrected. CCSD(T) is zero-point corrected with MP2 frequencies. [b] These are CCSD(T)/aug-cc-pVTZ, frozen-core single points, zero-point corrected with MP2/TZ2Pf+dif frequencies.

The density functionals do not perform nearly as well for the net activation energy, $E^b_{F,F}$. It is apparent that the functionals are underestimating the energy of the transition state, resulting in qualitatively incorrect barriers. Here, a significant split between the hybrid B3LYP functional and the pure BLYP and BP86 functionals is seen. B3LYP is typically 3−4 kcal mol^{-1} closer to the standard CCSD(T) value than the BLYP and BP86 functionals. However, B3LYP is still 1−3 kcal mol^{-1} smaller than the CCSD(T) reference. Near the 0.0 kcal mol^{-1} region, a difference of 2 kcal mol^{-1} in the barrier can affect the elementary rate constant for S_N2 displacement by orders of magnitude. In summary, the net activation barrier for the $CH_3F + F^-$ identity exchange reaction is predicted by TZ2Pf+dif CCSD(T) theory to be −0.53 kcal mol^{-1}, well within 1 kcal mol^{-1} of other rigorous ab initio values.[31,39] Compared to this benchmark, the pure DFT methods place the S_N2 transition state 6 kcal mol^{-1} too low, a striking error which is partially reduced (by roughly 60%) with the hybrid B3LYP scheme.

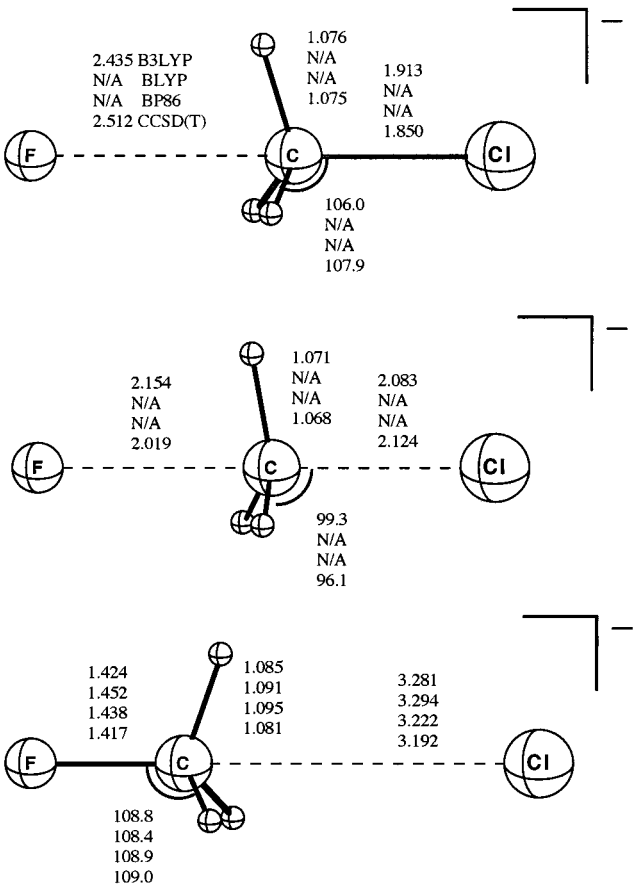

Figure 5. Geometries of the ion−molecule complex and transition state for the reaction $CH_3Cl + F^-$ using the TZ2Pf+dif basis set. All bond distances are in Å and bond angles in degrees. All structures are in C_{3v} symmetry. N/A signifies that the method did not yield a stationary point of the given type (see text for details.)

C. $CH_3Cl + F^- \rightarrow CH_3F + Cl^-$. The nonidentity exchange reaction with the Cl^- leaving group is also highly studied.[1,5,12,21,27,34,93,96,98,99] Previous definitive theoretical work was performed by Botschwina, Horn, Seeger and Oswald.[34] Their work includes optimizations of all structures with a basis set using the *spdf* space of aug-cc-pVQZ for carbon, fluorine and chlorine, and the *sp* space of aug-cc-pVQZ combined with the *d* space of aug-cc-pVTZ for hydrogen. Later single-point calculations utilized two sets of aug-cc-pVQZ *g* functions for fluorine and chlorine, and one set of cc-pVQZ *g* functions for carbon.

The structures for the stationary points along the reaction coordinate are detailed in Figure 5. Of immediate importance is the fact that the pure BLYP and BP86 functionals do not compute a double well potential at all for this reaction! With BLYP and BP86 there is no transition state and no $F^-\cdot H_3CCl$ structure, instead a monotonic descent to the product ion-molecule complex. We confirmed that the two pure functionals did not have these structures by following steepest descent paths from numerous starting points. In all of the cases, there was unimpeded collapse to the $FCH_3\cdot Cl^-$ structure.

The structure of the ion−molecule complex $F^-\cdot H_3CCl$ is analogous in topology to the $F^-\cdot H_3CF$ complex. Again the permanent charge on F^- is attracted to the permanent dipole of CH_3Cl, forming a C_{3v} complex. The deviation between B3LYP and the CCSD(T) reference is most significant in the heavy atom bond distances. B3LYP underestimates the F^-−C distance by 0.077 Å and overestimates the C−Cl bond distance by 0.063 Å. The C−Cl bond distance is increased by approximately 0.07

TABLE 4: Energetics (kcal mol^{-1}) of the $CH_3Cl + F^- \rightarrow CH_3F + Cl^-$ Reaction[a]

	$E^b_{F,Cl}$	$E^w_{F,Cl}$	$E^*_{F,Cl}$	$E^b_{Cl,F}$	$E^w_{Cl,F}$	$E^*_{Cl,F}$	$E^0_{F,Cl}$
				DZP + dif			
B3LYP	−14.73	−15.44	0.71	19.48	−8.43	27.90	−34.21
BLYP					−8.19		−31.28
BP86					−8.12		−32.15
CCSD(T)	−8.46	−13.91	5.45	21.07	−9.78	30.85	−29.54
				TZ2P + dif			
B3LYP	−15.82	−16.09	0.27	17.35	−8.27	25.62	−33.16
BLYP					−8.08		−30.18
BP86					−8.04		−30.72
CCSD(T)	−12.72	−15.36	2.64	16.14	−9.83	25.97	−28.86
				TZ2Pf + dif			
B3LYP	−15.29(−15.43)	−15.85(−15.85)	0.56(0.42)	17.82(16.76)	−8.34(−8.20)	26.19(24.96)	−33.11(−32.19)
BLYP					−8.25(−8.14)		−30.12(−29.28)
BP86					−8.19(−8.11)		−30.69(−29.84)
CCSD(T)	−11.28(−11.16)	−14.97(−14.85)	3.70(3.68)	18.24(17.34)	−9.83(−9.61)	28.07(26.95)	−29.52(−28.51)
aug-cc-pVTZ[b]	(−13.04)	(−15.92)	(2.88)	(18.17)	(−9.54)	(27.71)	(−31.22)
experiment							−33.8

[a] The numbers in parentheses are zero-point corrected. CCSD(T) is zero-point corrected with MP2 frequencies. [b] These are CCSD(T)/aug-cc-pVTZ, frozen-core single points, zero-point corrected with MP2/TZ2Pf+dif frequencies.

Å over isolated CH_3Cl (again with minimal change in the bond angle). The B3LYP bond angle is 1.9° smaller than the CCSD(T) reference. Our CCSD(T)/TZ2Pf+dif values are in excellent agreement with the Botschwina[34] values, which are $r_{F-C} = 2.502$ Å, $r_{C-Cl} = 1.853$ Å, $r_{C-H} = 1.080$ Å, and $\theta_{H-C-Cl} = 107.6°$.

The transition state calculations show larger overall deviations between B3LYP and CCSD(T). The F−C bond distance deviation is 0.135 Å, whereas the C−Cl deviation is 0.041 Å. Here, we also find a 3.2° deviation for θ_{H-C-Cl}. The CCSD(T)/TZ2Pf+dif values are again in fine agreement with the Botschwina[34] values of $r_{F-C} = 2.030$ Å, $r_{C-Cl} = 2.121$ Å, $r_{C-H} = 1.072$ Å, and $\theta_{H-C-Cl} = 96.3°$.

Last, the $FCH_3 \cdot Cl^-$ structure is considered, which is given as a stationary point by all of the functionals. This structure is analogous in form to the previous $F^- \cdot H_3CCl$ structure, with the roles of F and Cl reversed. We find that the r_{F-C} deviations are in the 0.007−0.035 Å range, but the r_{C-Cl} deviations are much more sizable, as large as 0.102 Å for BLYP. The largest bond angle deviation is 0.6° for BLYP. For the product complex, the C−F distance is only elongated by about 0.03 Å when compared to isolated CH_3F. As before, the CCSD(T)/TZ2Pf+dif values are in excellent agreement with the Botschwina[34] structural parameters, $r_{F-C} = 1.418$ Å, $r_{C-Cl} = 3.188$ Å, $r_{C-H} = 1.086$ Å, and $\theta_{F-C-H} = 108.9°$.

Table 4 lists the energetics of the F^-/Cl^- S_N2 reaction. There is generally good agreement for the complexation energies. For the forward reaction B3LYP is within 0.1 kcal mol^{-1} of the CCSD(T)/aug-cc-pVTZ result, and only 1 kcal mol^{-1} larger than the corresponding TZ2Pf+dif value. For the reverse reaction, both the aug-cc-pVTZ and the TZ2Pf+dif values are about 1.5 kcal mol^{-1} larger than the density functional values. Our CCSD(T)/aug-cc-pVTZ value of −15.92 kcal mol^{-1} for $E^w_{F,Cl}$ is less than 0.2 kcal mol^{-1} larger than the Botschwina et al.[34] value (−15.80 kcal mol^{-1}). The TZ2Pf+dif basis set yields a CCSD(T) value about 1 kcal mol^{-1} smaller. For the reverse reaction, Botschwina et al. predict $E^w_{Cl,F}$ to be −9.61 kcal mol^{-1}, in precise agreement with both our TZ2Pf+dif and aug-cc-pVTZ CCSD(T) values. Using their W1′-core method, Parthiban et al.[39] compute $E^w_{F,Cl} = -15.43$ kcal mol^{-1}, and $E^w_{Cl,F} = -9.51$ kcal mol^{-1}.

As in the fluoride system, the density functional methods employed here are not able to describe the net activation energies with the same type of accuracy, at least for the forward reaction. The deviation between B3LYP and CCSD(T) for $E^b_{F,Cl}$ is over 2 kcal mol^{-1} with the aug-cc-pVTZ basis set, and over 4 kcal mol^{-1} for the TZ2Pf+dif basis. The values for the reverse reaction, $E^b_{Cl,F}$, are more favorable for B3LYP, with a deviation of approximately 1.4 kcal mol^{-1} for the aug-cc-pVTZ results and 0.7 kcal mol^{-1} for the TZ2Pf+dif calculations. The inability of the pure functionals to compute a double well reaction profile is a critical flaw. In addition, the error in B3LYP for the intrinsic activation barrier for the forward reaction, $E^*_{F,Cl}$, must be emphasized. B3LYP gives it as only 0.42 kcal mol^{-1}, a very small activation barrier, which would anomalously affect the associated dynamics of this reaction.

The data in Table 4 reveal some substantial changes in the CCSD(T) energetics when the TZ2Pf+dif basis is replaced by aug-cc-pVTZ: $E^b_{F,Cl}$, −11.16 → −13.04 kcal mol^{-1}; $E^b_{Cl,F}$, 17.34 → 18.17 kcal mol^{-1}; and $E^0_{F,Cl}$, −28.51 → −31.22 kcal mol^{-1}. In these cases, the aug-cc-pVTZ results compare much more favorably with the high quality results of refs 34, 39: $E^b_{F,Cl}$, (−12.75, − 12.54); $E^b_{Cl,F}$, (20.17, 20.11); and $E^0_{F,Cl}$ (−32.92, − 32.65). Moreover, the 2.7 kcal mol^{-1} TZ2Pf+dif → aug-cc-pVTZ increase in the reaction exothermicity largely resolves the disparity with the experimental value, $E^0_{F,Cl} = -33.8$ kcal mol^{-1}. The problem in the TZ2Pf+dif basis can be isolated to the chlorine atom description.

In brief, the aug-cc-pVTZ basis set is a better choice for the energetics associated with the stationary points of the X = Cl reaction. However, comparison of the CCSD(T)/TZ2Pf+dif structures to those of the Botschwina et al.[34] shows the TZ2Pf+dif geometric parameters still to be of high quality. Some sizable r_{X-Y} deviations are present in this system, most particularly for weakly bound r_{F-C} distances. When compared to CCSD(T)/aug-cc-pVTZ, the density functional energetics are adequate for E^w and E^0, but lacking for E^b and E^*. In particular, the pure functionals are unable to yield a double well potential for this reaction.

D. $CH_3CN + F^- \rightarrow CH_3F + CN^-$. The reaction of acetonitrile with the fluoride anion has not been as widely studied in the literature as the previous two reactions, but still has a thorough literature,[2,105−108] the best work being a series of MP2/6-31++G** computations by Shi et al.[27,98,99] The structures for the stationary points are detailed in Figure 6. It is immediately noticed that the first ion−molecule complex, $F^- \cdot H_3CCN$, in C_s symmetry, does not have the fluoride anion

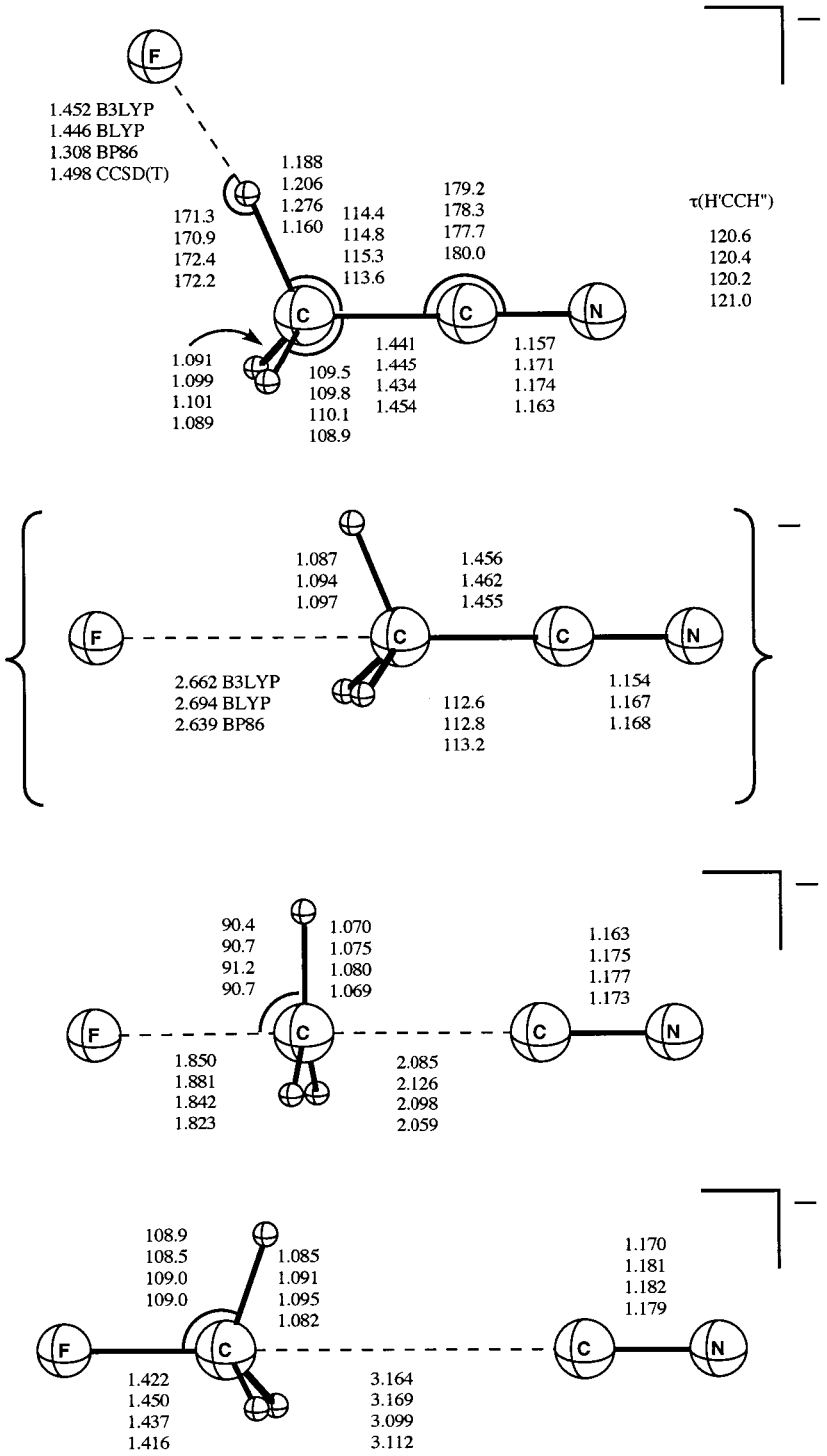

Figure 6. Geometries of the ion−molecule complexes, transition state, and second-order saddle point (inside braces) for the reacion of $CH_3CN + F^-$ using the TZ2Pf+dif bais set. All bond distances are in Å, bond and torsional angles in degrees. The top structure is C_s symmetry, whereas the bottom three are C_{3v} symmetry. For (H′, H″) definitions, see caption to Figure 3.

on the C−C axis. Instead, the fluoride anion is attached to a single hydrogen, with the cyano group slightly bent toward the fluoride. The previous work by Shi[27] assumed a collinear attack, i.e., a C_{3v} ion−molecule complex. We performed some preliminary tests on the collinear ion−molecule complex, and determined the C_{3v} structure to be a second-order saddle point. The earlier work by Yamabe et al.[107] showed that the C_s structure was lower in energy than the linear C_{3v} case by more than 2 kcal mol^{-1} at the SCF level with a modified 4-31G basis. They concluded that the collinear structure involves predominantly electrostatic interactions, i.e., "three $F^{-1}\cdots H^{\delta+}$ attractions", whereas the C_s species exhibits a semi-covalent hydrogen bond.

The collinear C_{3v} structure was examined here with the three density functional methods, utilizing the TZ2Pf+dif basis set. It was determined to be a second-order saddle point, with a doubly degenerate imaginary frequency for F−C−C bending of $80i-100i$ cm^{-1}. The structure is depicted in braces in Figure 6, below one of the equivalent C_s minima. A large r_{F-C} bond distance of about 2.66 Å is exhibited. The acetonitrile geometry is virtually unchanged compared with isolated acetonitrile, with only θ_{C-C-H} appreciably changed by about 2.5°. Energetically,

TABLE 5: Energetics (kcal mol^{-1}) of the $CH_3CN + F^- \rightarrow CH_3F + CN^-$ Reaction[a]

	$E^b_{F,CN}$	$E^w_{F,CN}$	$E^*_{F,CN}$	$E^b_{CN,F}$	$E^w_{CN,F}$	$E^*_{CN,F}$	$E^0_{F,CN}$
				DZP + dif			
B3LYP	13.12	−24.90	38.02	9.78	−8.43	18.21	3.34
BLYP	10.15	−25.31	35.47	5.30	−8.22	13.52	4.85
BP86	10.66	−27.70	38.35	5.33	−8.11	13.44	5.32
CCSD(T)	16.38	−22.58	38.96	13.42	−9.05	22.47	2.96
				TZ2P + dif			
B3LYP	12.74	−24.55	37.29	9.14	−7.89	17.03	3.61
BLYP	10.11	−24.65	34.77	4.55	−7.74	12.29	5.57
BP86	10.30	−27.27	37.57	4.68	−7.71	12.39	5.61
CCSD(T)	13.41	−23.08	36.49	10.01	−8.84	18.85	3.40
				TZ2Pf + dif			
B3LYP	13.19(12.56)	−24.69(−25.54)	37.87(38.10)	10.09(10.25)	−7.77(−7.36)	17.86(17.60)	3.10(2.32)
BLYP	10.53(9.74)	−24.80(−25.76)	35.32(35.50)	5.39(5.42)	−7.60(−7.24)	12.99(12.66)	5.13(4.32)
BP86	10.68(9.91)	−27.56(−29.26)	38.24(39.17)	5.57(5.58)	−7.57(−7.23)	13.14(12.81)	5.11(4.33)
CCSD(T)	14.68(14.27)	−23.81(−24.48)	38.49(38.74)	12.04(12.17)	−8.72(−8.32)	20.76(20.50)	2.64(2.09)
aug-cc-pVTZ[b]	(12.54)	(−25.08)	(37.62)	(11.80)	(−8.68)	(20.48)	(0.74)
experiment							1.7

[a] The numbers in parentheses are zero-point corrected. CCSD(T) is zero-point corrected with MP2 frequencies. [b] These are CCSD(T)/aug-cc-pVTZ, frozen-core single points, zero-point corrected with MP2/TZ2Pf+dif frequencies.

the C_{3v} structure is 6.50, 7.13, and 9.25 kcal mol^{-1} higher in energy than the C_s form for the B3LYP, BLYP, and BP86 methods, respectively (with the TZ2Pf+dif basis set). This is a much larger difference than the 2 kcal mol^{-1} predicted by SCF/4-31G,[107] but may be readily explained by the better treatment that the density functionals and the inclusion of diffuse and polarization functions provide.

For the structural quantities of the C_s ion−molecule complex, BP86 performs very poorly. It has the worst bond distance deviations, 0.19 Å for r_{F-H} and 0.02 Å for r_{C-C}. It also has the largest angle deviations, 1.7° for $\theta_{H'-C-C}$ and 0.8° for $\tau_{H'-C-C-H''}$. B3LYP again performs the best among the three functionals, averaging about half the deviation of the pure functionals.

Continuing the trend for the previous reactions, larger deviations among the methods arise for the $[F-CH_3-CN]^{-\ddagger}$ transition state, in C_{3v} symmetry. For r_{X-Y} deviations the three density functionals deviate from the CCSD(T) standard in average by more than 0.025 Å, the pure functionals again performing worst. For r_{F-C} the deviations are substantial, with BLYP having the largest, 0.058 Å. The previous work of Shi et al.[27] is in qualitative agreement with our findings, describing a similar topology.

Last, the $FCH_3 \cdot CN^-$ ion−molecule complex is considered, having C_{3v} symmetry. This complex has a structure similar to the ion−molecule complexes of the F and Cl systems, complexes which are predominantly electrostatic. The r_{C-F} distance is increased by about 0.03 Å compared to isolated CH_3F. B3LYP is best in predicting r_{X-H}, with a deviation of only 0.003 Å. However, for r_{X-Y}, BP86 does best. The largest deviation is in the long r_{C-C} bond, 0.057 Å for BLYP. Surprisingly, BP86 is much closer for this bond distance.

The energetics of this reaction, listed in Table 5, are now considered. For both the forward and the reverse reaction we see good agreement between the aug-cc-pVTZ and TZ2Pf+dif CCSD(T) complexation energies, both within 0.6 kcal mol^{-1} of each other. For the forward reaction, the density functionals consistently predict larger complexation energies. BP86 is largest, calculating a very substantial 4.18 kcal mol^{-1} larger value than CCSD(T). For the reverse reactions, the opposite is the case, namely, that the functionals consistently give complexation energies smaller than CCSD(T). Here, however, all three functionals cluster together, with the largest DFT deviation (BP86) being 1.45 kcal mol^{-1}. Because of their different geometry for $F^- \cdot H_3CCN$ (C_{3v}), precise comparisons between the Shi et al.[27] $E^w_{C,CN}$ values and the present CCSD(T)/TZ2Pf+dif results are not possible. Instead, we can compare analogous values for the second-order saddle point. For the binding energy of this collinear complex, MP2/6-31++G**//RHF/6-31++G** theory yields 17.49 kcal mol^{-1},[27] close to our values of 18.41 kcal mol^{-1}, 17.97 kcal mol^{-1}, and 18.71 kcal mol^{-1} for B3LYP, BLYP, and BP86 respectively, using the TZ2Pf+dif basis set. For $E^w_{CN,F}$, a direct comparison is possible, and the same MP2 method gives a complexation energy of 8.92 kcal mol^{-1}, within 1 kcal mol^{-1} of our CCSD(T)/aug-cc-pVTZ and CCSD(T)/TZ2Pf+dif values of 8.68 and 8.32 kcal mol^{-1}, respectively.

For the net activation barrier we see the usual trend of B3LYP better approximating the CCSD(T) standard than the pure functionals, in this case by 3 kcal mol^{-1} for the forward reaction and 4.5 kcal mol^{-1} for the reverse. For the forward reaction, B3LYP/TZ2Pf+dif is in excellent agreement with the CCSD(T)/aug-cc-pVTZ computation, deviating by only 0.02 kcal mol^{-1}. For the reverse reaction, it deviates by 1.55 kcal mol^{-1} when compared to CCSD(T)/aug-cc-pVTZ. The coupled cluster calculations are in good agreement for the reverse reaction; however, for the forward reaction TZ2Pf+dif computes an $E^b_{F,CN}$ value 1.73 kcal mol^{-1} larger than aug-cc-pVTZ. The pure functionals are systematically poor in describing E^b, deviating by 2.5−3.0 kcal mol^{-1} for the forward reaction, and over 6 kcal mol^{-1} for the reverse, when compared to the aug-cc-pVTZ reference. Shi et al.[27] compute $E^b_{F,CN}$ to be 19.62 kcal mol^{-1}, in poor agreement with our computed value of 12.54 and 14.27 for aug-cc-pVTZ and TZ2Pf+dif. For the reverse reaction, the Shi et al. value of 11.67 kcal mol^{-1} compares very favorably to our CCSD(T)/aug-cc-pVTZ and CCSD(T)/TZ2Pf+dif computations of 11.80 and 12.17 kcal mol^{-1}, respectively.

For the reaction energy, we find the aug-cc-pVTZ and TZ2Pf+dif results deviating by 1.35 kcal mol^{-1}. Again, B3LYP does best in approximating the coupled cluster values, whereas the pure functionals are 2.0−3.5 kcal mol^{-1} too large. Utilizing the experimental heats of formation, we compute $E^0_{F,CN}$ to be 1.7 kcal mol^{-1}, in good agreement with our coupled cluster values.

In summary, although the $CH_3CN + F^-$ system has an electrostatic, collinear product complex, its reactant complex

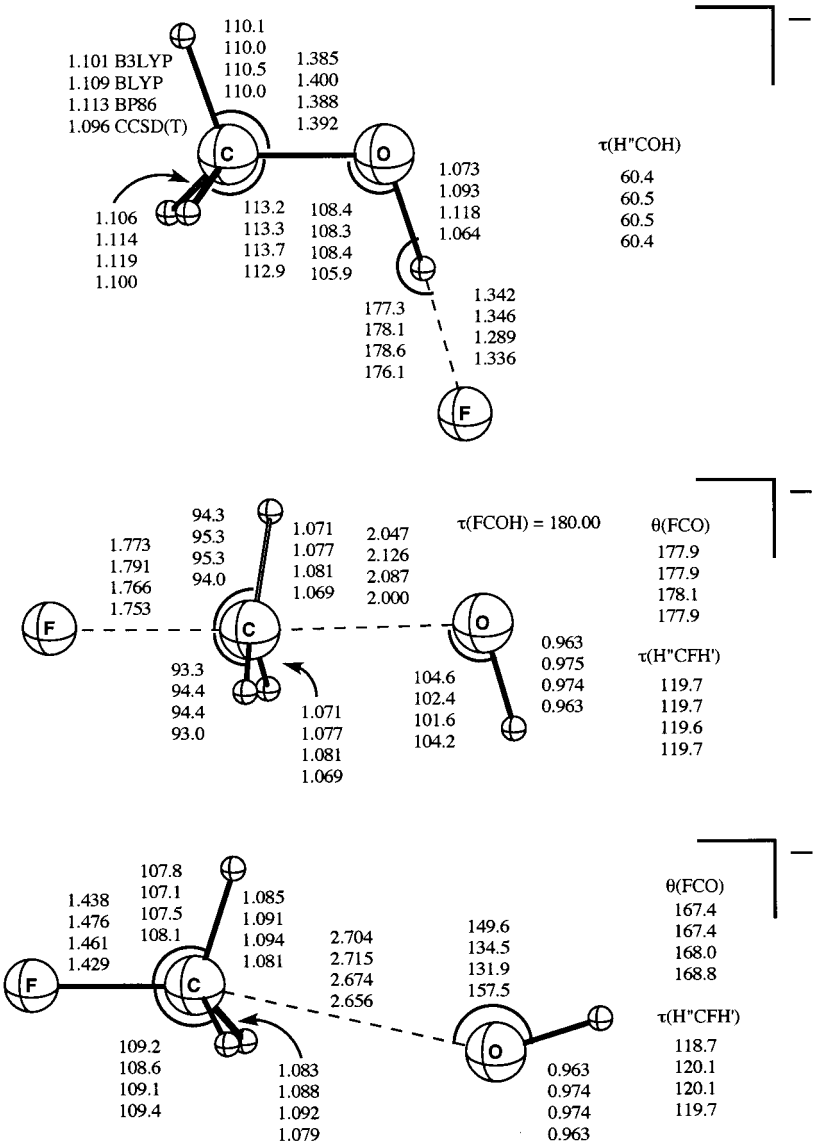

Figure 7. Geometries of the ion−molecule complexes and transition state for the reaction of $CH_3OH + F^-$ using the TZ2Pf+dif basis set. All bond distances are in Å, bond and torsional angles in degrees. All structures are C_s symmetry. For (H′, H″) definitions see caption to Figure 3.

displays a strong, single, semi-covalent hydrogen bond (25 kcal mol^{-1}) with increased stabilization of about 10 kcal mol^{-1} over its electrostatic, collinear alternative. The DFT methods studied here provide the correct topology of the surface and give complexation energies accurate to 2 kcal mol^{-1}, except for the failure of BP86 for $E^w_{F,CN}$. However, for the forward and reverse activation barriers, only B3LYP is reliable to 2 kcal mol^{-1}, and the pure functionals severely underestimate the height of the transition state.

E. $CH_3OH + F^- \rightarrow CH_3F + OH^-$. The reaction of methanol with fluoride has been previously investigated in the literature,[4,95,96,98,99,105,106,108−110] with the best theoretical works being an MP2/6-311++G(3dp,3df) study by Riveros et al.,[111] a CISD/TZP+dif investigation by Wladkowski et al.[112] (only on $CH_3OH{\cdot}F^-$), and the previously cited MP2/6-31++G** paper by Shi et al.[27]

The structures for the stationary points are detailed in Figure 7. The reactant $CH_3OH{\cdot}F^-$ ion−molecule complex is the first one considered here that does not arise from "backside attack". Instead of being closest to the methyl carbon, fluoride is attracted to the more acidic hydroxyl hydrogen. We attempted, to no avail, to find a stationary point with the fluoride anion attached to the methyl hydrogens. The potential surface was carefully scanned on the periphery of the methyl group, eliminating the possibility of a backside stationary point. In addition, a B3LYP/DZP+dif IRC computation was performed following the S_N2 reaction coordinate backward toward reactants, and the system continuously evolved to $CH_3OH{\cdot}F^-$.

For the $CH_3OH{\cdot}F^-$complex an r_{H-F} distance of approximately 1.3 Å was computed, in comparison with the 0.917 Å of isolated HF.[113] This type of structure indicates a larger charge-transfer effect. Mulliken analysis utilizing the TZ2Pf+dif basis set computes the charge on the fluorine atom to be about −0.9. Wladkowski et al.[112] describe it as, "... the large fluoride affinity of methanol is ultimately realized only after charge transfer and higher-order mixing occur". In general for this molecule BP86 performs poorly, with the worst deviation being that of r_{O-H} at 0.054 Å. BP86 is also the only functional with poor performance for r_{H-F}, deviating by almost 0.05 Å. For r_{C-O}, all density functional methods deviate from CCSD(T) by less than 0.01 Å. For the bond angles, again B3LYP performs the best, but it still deviates by over a degree for two bond angles, θ_{C-O-H} and θ_{O-H-F}. The values for the torsional angle $\tau_{H''-C-O-H}$ are all within 0.1° of the reference. The previous work of Shi et

TABLE 6: Energetics (kcal mol^{-1}) of the $CH_3OH + F^- \rightarrow CH_3F + OH^-$ Reaction[a]

	$E^b_{F,OH}$	$E^w_{F,OH}$	$E^*_{F,OH}$	$E^b_{OH,F}$	$E^w_{OH,F}$	$E^*_{OH,F}$	$E^0_{F,OH}$
				DZP + dif			
B3LYP	16.91	−29.81	46.71	−4.57	−13.15	8.58	21.47
BLYP	11.78	−29.42	41.20	−8.31	−12.95	4.63	20.09
BP86	12.71	−31.55	44.06	−7.80	−12.78	4.98	20.51
CCSD(T)	20.37	−29.68	50.05	−1.98	−14.21	12.24	22.34
				TZ2P + dif			
B3LYP	15.07	−29.08	44.15	−5.76	−12.75	6.99	20.83
BLYP	10.14	−28.50	38.63	−9.46	−12.71	3.25	19.60
BP86	10.93	−30.62	41.55	−9.02	−12.53	3.52	19.95
CCSD(T)	16.51	−28.90	45.41	−4.80	−13.87	9.08	21.31
				TZ2Pf + dif			
B3LYP	15.58(14.15)	−29.35(−30.05)	44.93(44.21)	−4.83(−4.10)	−12.60(−11.96)	7.77(7.86)	20.40(18.26)
BLYP	10.60(8.99)	−28.77(−29.65)	39.38(38.64)	−8.63(−8.14)	−12.49(−11.93)	3.86(3.78)	19.23(17.14)
BP86	11.37(9.80)	−30.95(−32.13)	42.32(41.93)	−8.16(−7.63)	−12.32(−11.85)	4.16(4.22)	19.53(17.43)
CCSD(T)	17.76(16.47)	−30.08(−30.63)	47.84(47.10)	−3.05(−2.22)	−13.78(−13.01)	10.73(10.79)	20.80(18.69)
aug-cc-pVTZ[b]	(15.20)	(−30.97)	(46.17)	(−2.26)	(−13.14)	(10.88)	(17.46)
experiment							17.7

[a] The numbers in parentheses are zero-point corrected. CCSD(T) is zero-point corrected with MP2 frequencies. [b] These are CCSD(T)/aug-cc-pVTZ, frozen-core single points, zero-point corrected with MP2/TZ2Pf+dif frequencies.

al.[27] cannot be compared to the present results because of their assumed collinear backside attack. It should be noted that B3LYP does very well for all coordinates, save θ_{C-O-H}.

The $[F-CH_3-OH]^{-\ddagger}$ transition state has a slightly nonlinear F−C−O framework, θ_{F-C-O} being about 178°, with oxygen pushed up slightly toward the unique hydrogen. The methyl hydrogens are slightly pyramidalized toward the hydroxyl group. B3LYP does very well for the r_{X-H} values, with deviations on the order of 0.002 Å. The pure functionals average deviations of about 0.012 Å for the same quantities. However, there is poor agreement with the reference method for r_{X-Y}. B3LYP still performs best, but has deviations of 0.020 Å for r_{F-C} and 0.047 Å for r_{C-O}. The pure functionals are even worse! The largest deviation is 0.126 Å for BLYP r_{C-O}. For the bond angle deviations, we again find B3LYP systematically outperforming the pure functionals. BLYP and BP86 do not perform adequately for θ_{C-O-H}, deviating by 1.8° and 2.6°, respectively. We find excellent agreement among all the methods for $\tau_{H''-C-F-H'}$. Riveros et al.[111] agree qualitatively with our results, whereas the assumed collinear F−C−O framework of Shi et al.[27] is close, but not correct.

Last, the $FCH_3 \cdot OH^-$ ion−molecule complex is considered. This species has the hydroxyl group pushed down, toward the mirrored hydrogens. The r_{C-F} distance is increased by 0.04−0.06 Å compared to isolated CH_3F. For the r_{X-Y} values B3LYP generally outperforms BLYP and BP86. The worst r_{X-H} deviation is 0.013 Å for the BP86 $r_{C-H'}$ value. For r_{X-Y} B3LYP is within 0.01 Å of the CCSD(T) reference for r_{C-F}, but no other r_{X-Y} deviation is under 0.01 Å, whereas the largest deviation is the BLYP r_{C-O} overestimation of 0.059 Å. For the bond angles, we immediately observe a huge deviation among the methods in the θ_{C-O-H} angle. BLYP and BP86 are both 23°−25° smaller than the CCSD(T) value, while B3LYP underevaluates the angle by 8°. The potential energy surface is very flat with respect to θ_{C-O-H}. It only requires 0.50 kcal mol^{-1} to make $\theta_{C-O-H} = 180°$ (B3LYP/TZ2Pf+dif level, freezing all other coordinates). For $\tau_{H''-C-F-H'}$, all DFT values deviate for the reference by no more than 1°. Again Riveros et al.[111] is in qualitative agreement with our structures, whereas the Shi et al.[27] structures are not correct.

We now consider the energetics of this reaction, listed in Table 6. The two coupled cluster references are in very good agreement for the complexation energies. The density functionals are consistently within 1.5 kcal mol^{-1} of the CCSD(T) standard for both the forward and reverse reaction. The Riveros et al.[111] values of $E^w_{F,OH} = -32.4$ kcal mol^{-1} and $E^w_{OH,F} = -13.6$ kcal mol^{-1} compare favorably with the CCSD(T) values computed here. The assumed collinear structures of Shi et al.[27] produce large errors. The MP2/6-311++G**-computed $E^w_{F,OH} = -8.59$ kcal mol^{-1} is over 20 kcal mol^{-1} smaller in magnitude than the actual reactant complexation energy, whereas their collinear $E^w_{OH,F} = -14.54$ kcal mol^{-1} is about 1.5 kcal mol^{-1} too negative, despite use of an unrelaxed structure.

Use of the aug-cc-pVTZ basis set lowers the forward net activation barrier ($E^b_{F,OH}$) by 1.27 kcal mol^{-1}. The corresponding change in the reverse barrier is negligible. Continuing the previous pattern, the density functionals do not describe the net activation barriers with the same accuracy as the complexation energies. For both the forward and the reverse reaction B3LYP is within 1.9 kcal mol^{-1} of CCSD(T)/aug-cc-pVTZ, whereas the pure functionals undercompute the barrier by over 5 kcal mol^{-1}. The Riveros et al.[111] values of $E^b_{F,OH} = 16.4$ kcal mol^{-1} and $E^b_{OH,F} = -1.3$ kcal mol^{-1} compare very favorably with the present CCSD(T) results. The Shi et al.[27] results, $E^b_{F,OH} = 19.16$ kcal mol^{-1} and $E^b_{OH,F} = -4.37$ kcal mol^{-1} appear to be off by 2−4 kcal mol^{-1}, but are not drastically affected by assumed F−C−O linearity, which amounts to only 2° error.

We see good agreement for all of the methods for the reaction energy, with the density functionals never deviating for any basis set from the standard by more than 2.25 kcal mol^{-1}. With the CCSD(T) method the aug-cc-pVTZ basis set computes a reaction energy 1.23 kcal mol^{-1} smaller than TZ2Pf+dif. In comparison to the experimental $E^0_{F,OH}$ of 17.7 kcal mol^{-1}, all of our methods perform well, within 1 kcal mol^{-1}. The Riveros et al.[111] endoergicity of $E^0_{F,OH} = 17.7$ kcal mol^{-1} again compares very favorably with the present values, in contrast to the Shi et al.[27] value of 23.5 kcal mol^{-1} (MP2/6-31++G**).

To summarize, the $CH_3OH + F^-$ system is the first encountered here without a reactant complex for backside attack, rather a $CH_3OH \cdot F^-$ complex with a very strong (31 kcal mol^{-1}) semicovalent bond to the acidic hydroxyl hydrogen. In contrast, the product complex, $FCH_3 \cdot OH^-$, is a typical ion−dipole adduct, albeit with a loose C−O−H bending mode. For both complexes, the DFT binding energies are accurate to 1.5 kcal mol^{-1},

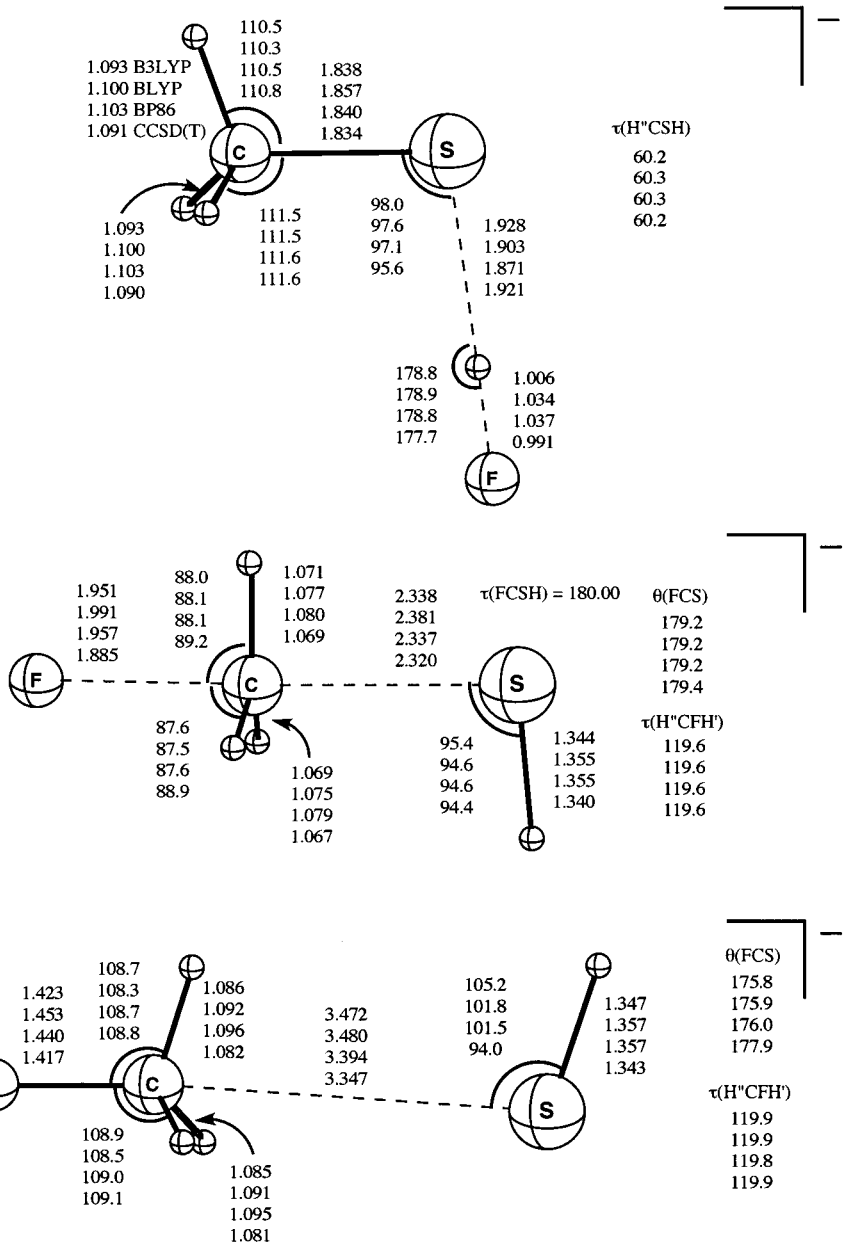

Figure 8. Geometries of the ion−molecule complexes and transition state for the reaction $CH_3SH + F^-$ using the TZ2Pf+dif basis set. All bond distances are in Å, bond and torsional angles in degrees. All structures are in C_s symmetry. For (H′, H″) definitions see caption to Figure 3.

although there is some difficulty in predicting structural parameters such as θ_{C-O-H} in $FCH_3{\cdot}OH^-$. For the $E^b_{F,OH}$ and $E^b_{OH,F}$ barriers, B3LYP is too low by less than 2 kcal mol^{-1}, but BLYP and BP86 fail by predicting values greater than 5 kcal mol^{-1} too low.

F. $CH_3SH + F^- \rightarrow CH_3F + SH^-$. The reaction of methanethiol and fluoride is not as thoroughly studied in the literature[4,98,106] as the previous reactions. The best published theoretical work is the MP2/6-31++G** analysis of Shi et al.[27] The structures for the stationary points are detailed in Figure 8. The $CH_3SH{\cdot}F^-$ ion−molecule complex is analogous in topology to the previous $CH_3OH{\cdot}F^-$complex, with the fluoride abstracting the thiol proton. In this case, however, the H−F bond distance is much shorter than in the methanol case, only 0.1 Å longer than the isolated HF bond (0.917 Å). The S−H distance is concomitantly elongated by between 0.5 and 0.6 Å. This type of structure is testament to a massive charge transfer; Mulliken analyses compute a CH_3S net charge of −0.84. The C−S bond is only slightly elongated by complexation, less than 0.02 Å. For the bond distances, again B3LYP consistently performs the best, with a maximum deviation of 0.015 Å, for r_{H-F}. For this same bond distance, BLYP and BP86 are over 0.04 Å too long. In addition BLYP does rather poorly for r_{C-S}, overestimating by 0.023 Å. For the bond angles, we find the functionals performing well for $\theta_{H'-C-S}$ and $\theta_{H''-C-S}$, usually deviating by less than 0.5°. For θ_{S-H-F} the funtionals all deviate by slightly over 1°, and for θ_{C-S-H} B3LYP and BLYP overestimate the angle by over 2°. We cannot directly compare with the Shi et al.[27] paper because they assumed linear backside attack.

The $[F-CH_3-SH]^{-‡}$ col has a slightly bent F−C−S framework, θ_{F-C-S} being about 179.2°, with the sulfur pushed up toward the unique methyl hydrogen. The methyl hydrogens are slightly pyramidalized toward the fluoride, which is the opposite of the $[F-CH_3-OH]^{-‡}$ case. For the r_{X-H} bond distances, B3LYP does well, with all deviations being under 0.004 Å. BP86 is the worst, with all r_{X-H} deviations being over 0.01 Å. For r_{C-S} B3LYP and BP86 are too large by 0.018 and 0.017 Å, respectively, but BLYP is over 0.06 Å too large. For the

TABLE 7: Energetics (kcal mol^{-1}) of the $CH_3SH + F^- \rightarrow CH_3F + SH^-$ Reaction[a]

	$E^b_{F,SH}$	$E^w_{F,SH}$	$E^*_{F,SH}$	$E^b_{SH,F}$	$E^w_{SH,F}$	$E^*_{SH,F}$	$E^0_{F,SH}$
				DZP + dif			
B3LYP	0.86	−36.36	37.21	11.76	−8.03	19.78	−10.90
BLYP	−2.78	−34.63	31.85	6.15	−7.89	14.04	−8.93
BP86	−2.90	−38.25	35.35	7.02	−7.90	14.92	−9.92
CCSD(T)	8.50	−32.83	41.33	13.27	−9.64	22.91	−4.77
				TZ2P + dif			
B3LYP	−0.57	−36.34	35.77	10.05	−7.72	17.77	−10.62
BLYP	−4.02	−34.46	30.44	4.58	−7.64	12.21	−8.59
BP86	−3.94	−37.93	33.98	5.32	−7.65	12.97	−9.26
CCSD(T)	3.98	−36.12	40.10	9.03	−9.60	18.63	−5.05
				TZ2Pf + dif			
B3LYP	0.02(−0.57)	−36.33(−35.53)	36.35(34.95)	11.03(10.91)	−7.57(−7.20)	18.60(18.11)	−11.01(−11.48)
BLYP	−3.49(−4.22)	−34.46(−33.97)	30.97(29.74)	5.44(5.23)	−7.46(−7.18)	12.90(12.41)	−8.93(−9.45)
BP86	−3.47(−4.14)	−37.96(−37.43)	34.49(33.29)	6.21(6.05)	−7.48(−7.21)	13.69(13.26)	−9.68(−10.19)
CCSD(T)	4.70(4.29)	−37.29(−36.43)	41.99(40.72)	11.21(11.18)	−9.58(−9.20)	20.80(20.38)	−6.52(−6.88)
aug-cc-pVTZ[b]	(1.57)	(−38.04)	(39.61)	(13.01)	(−8.60)	(21.61)	(−11.45)
experiment							−11.9

[a] The numbers in parentheses are zero-point corrected. CCSD(T) is zero-point corrected with MP2 frequencies. [b] These are CCSD(T)/aug-cc-pVTZ, frozen-core single points, zero-point corrected with MP2/TZ2Pf+dif frequencies.

r_{F-C} distance, the functionals all overshoot the CCSD(T) method by at least 0.065 Å, with BLYP being worst(0.106 Å). For the bond angles, deviations are generally significant, but under 1.3°.

As in the methanol case, for $FCH_3 \cdot SH^-$ the thiol sulfur is pushed down below the F−C axis, but unlike the methanol case, the thiol hydrogen is pushed up, toward the unique methyl hydrogen. It is immediately evident that the density functionals overcompute θ_{C-S-H}, calculating an angle 7−11° larger than the coupled cluster reference value. This occurrence is opposite the $FCH_3 \cdot OH^-$ case, where the DFT methods predict θ_{C-O-H} values much smaller than CCSD(T). As in the $FCH_3 \cdot OH^-$ product complex, the potential energy surface is flat for θ_{C-S-H} bending, only requiring 0.75 kcal mol^{-1} to become 180° (B3LYP/TZ2Pf+dif level, again freezing all other coordinates). For r_{C-S}, the density functional deviations are particulary large, with B3LYP and BP86 overestimating by over 0.12 Å. BP86 is better, but still deviates by 0.047 Å. We also find the functionals undercomputing θ_{F-C-S}, by 2°.

The energetics of this reaction are listed in Table 7. The aug-cc-pVTZ and TZ2Pf+dif coupled cluster complexation energies are within 0.6 kcal mol^{-1} of each other for the reverse reaction and 1.7 kcal mol^{-1} for the forward reaction. For the reverse reactions the density functionals are very tightly placed. The values of $E^w_{F,SH}$ are more variant, with a range of 3.5 kcal mol^{-1}. For the forward reaction BP86 is best, being within 1 kcal mol^{-1} of the CCSD(T)/aug-cc-pVTZ results. All of the functionals are 1.4 kcal mol^{-1} smaller than the aug-cc-pVTZ reference for the reverse reaction.

As we have seen previously, the density functionals do not describe the net activation barrier (E^b) well. For the forward reaction the usual trend of B3LYP outperforming BLYP and BP86 is evident, by 3−4 kcal mol^{-1} for the forward reaction, and 5−6 kcal mol^{-1} for the reverse reaction. B3LYP is still over 2 kcal mol^{-1} too small for both the forward and reverse CCSD(T)/aug-cc-pVTZ barrier. For $E^b_{F,SH}$ CCSD(T)/aug-cc-pVTZ computes a value 2.72 kcal mol^{-1} smaller than the TZ2Pf+dif value, while for $E^b_{SH,F}$ the aug-cc-pVTZ result is 1.83 kcal mol^{-1} larger.

The substantial difference between aug-cc-pVTZ and TZ2Pf+dif continues for $E^0_{F,SH}$, where aug-cc-pVTZ increases the exothermicity of the reaction by 4.57 kcal mol^{-1}. The aug-cc-pVTZ result is in much better agreement with the experimental value of −11.9 kcal mol^{-1}. B3LYP is also in very good agreement with this value, while the pure functionals are both within 2 kcal mol^{-1} of the aug-cc-pVTZ result. The poor TZ2Pf+dif result for $E^0_{F,SH}$ in wave function based computations is a consequence of substantial deficiencies in the sulfur TZ2Pf+dif basis.

In summary, the $CH_3SH + F^-$ surface has the same topology as for $CH_3OH + F^-$, but exhibits greater extremes. We find no evidence of a backside reactant complex, only a $CH_3SH \cdot F^-$adduct with a prodigious 38 kcal mol^{-1} binding energy and massive charge transfer (more like $CH_3S^- \cdot HF$). Despite some striking errors in geometric parameters, the DFT methods provide qualitatively correct structures and 2 kcal mol^{-1} accuracy in the complexation energies, except for BLYP $E^w_{F,SH}$. With the CCSD(T) method, it proves very important to supplant the TZ2Pf+dif basis with aug-cc-pVTZ to achieve barrier heights and a reaction exothermicity accurate to the 1 kcal mol^{-1} level. Compared to the aug-cc-pVTZ CCSD(T) standard, B3LYP provides a near perfect $E^0_{F,SH}$, but $E^b_{F,SH}$ and $E^b_{SH,F}$ barriers 2 kcal mol^{-1} too low. Once again, the pure functionals fail for the net activation barriers, undercomputing them by 5−8 kcal mol^{-1}.

G. $CH_3NH_2 + F^- \rightarrow CH_3F + NH_2^-$. The previous theoretical work on this reaction is not very recent,[2,27,95,98,99,105,106] and the MP2/6-31++G** results of Shi et al.[27] are the best available, although linear backside attack was assumed. The structures for the salient stationary points of the reaction are detailed in Figure 9. The $CH_3NH_2 \cdot F^-$ ion−molecule complex is the first of C_1 symmetry encountered here. Because there are 18 degrees of freedom for this species, both a depiction and a Newman projection are utilized to describe all of the internal coordinates. Due to its lack of symmetry, the CCSD(T) optimizations on the C_1 reactant complex were performed with the TZ2P+dif rather than the TZ2Pf+dif basis set. CCSD(T)/TZ2Pf+dif single-point calculations were performed at the CCSD(T)/TZ2P+dif optimized geometry. Rather than defining H, H′ and H″ hydrogens as before (caption of Figure 3), each hydrogen is indexed with a number. Instead of being in what was the H′−C−N plane in CH_3NH_2, the fluoride anion is connected to a single amine hydrogen. The H−F distance is about 0.7 Å longer than in isolated HF. It indicates modest charge transfer; in this case a TZ2Pf+dif Mulliken analysis indicates the fluoride charge to be −0.93. Meanwhile the corresponding N−H bond length is only slightly increased (about

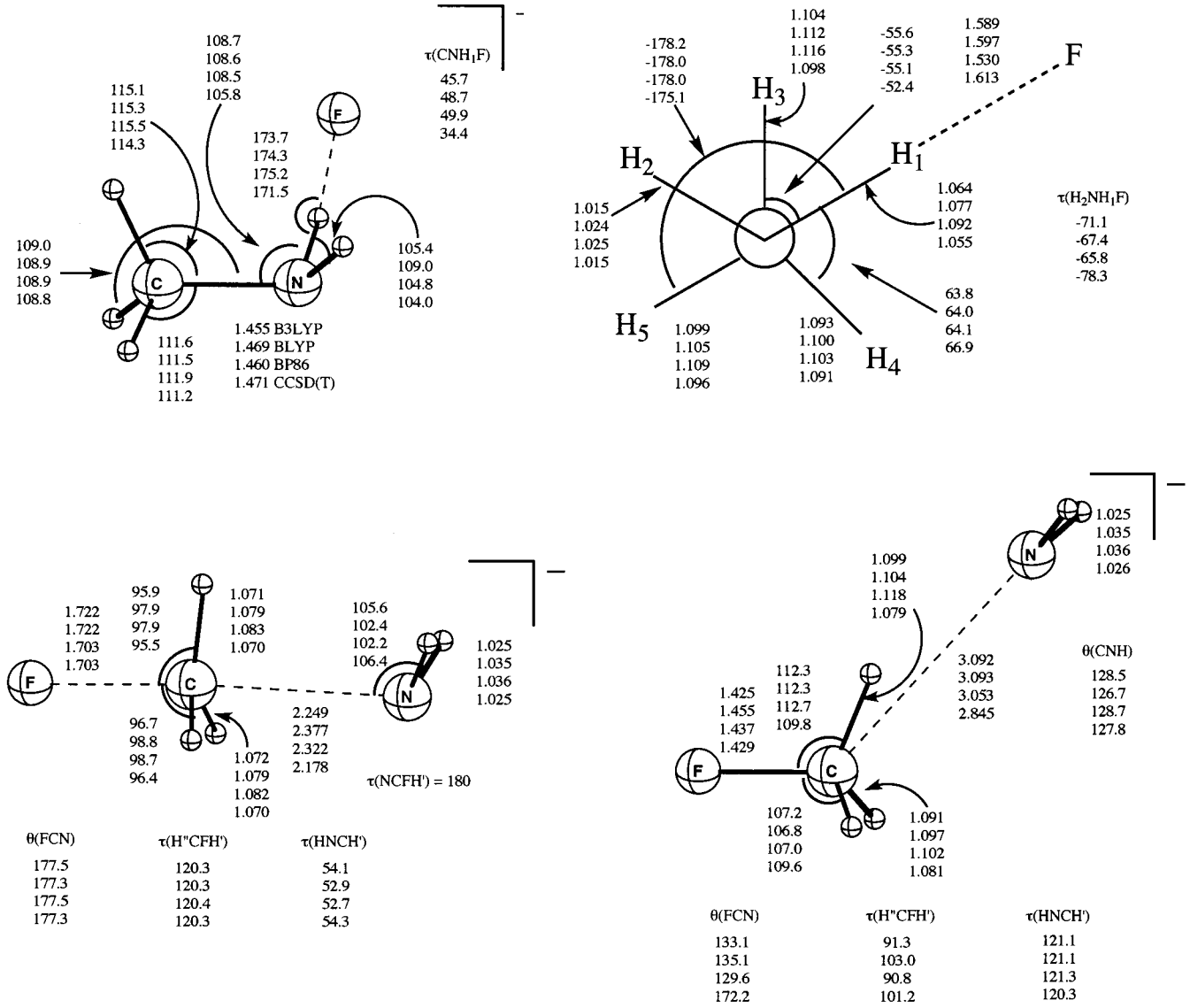

Figure 9. Geometries of the ion−molecule complexes and transition state for the reaction $CH_3NH_2 + F^-$ using the TZ2Pf+dif basis set. All bond distances are in Å, bond and torisional angles in degrees. The top structure is of C_1 symmetry, whereas the bottom two are of C_s symmetry. A Newmann diagram is provided to clarify the orientations in the C_1 molecule. For (H′, H″) definitions see caption to Figure 3. The CCSD(T) values for the C_1 ion−molecule complex use the TZ2P+dif basis set.

0.05 Å). Most of the deviations in r_{X-H} are small, under 0.01 Å. However, for r_{H_1-F} all the functionals deviate by over 0.01 Å, with BP86 displaying the largest deviation of 0.083 Å. There is only one r_{X-Y} for which B3LYP performs worst, with a deviation of 0.016 Å for r_{C-N}. For θ_{C-N-H_1} and θ_{N-H_1-F}, all of the deviations are over 2°, and for the torsional angles all are over 2.5°. The largest DFT torsional deviations are in τ_{C-N-H_1-F} and $\tau_{H_2-N-H_1-F}$, over 10°.

The $[F-CH_3-NH_2]^{-\ddagger}$ transition state, of C_s symmetry, has the amine nitrogen slightly pushed down toward the mirrored methyl hydrogens, with $\theta_{F-C-N} = 177.3°$. The methyl hydrogens are slightly pyramidalized toward the amine group. Extremely large deviations in r_{N-C} are manifested, with B3LYP overestimating by 0.071 Å, whereas BLYP and BP86 are 0.199 and 0.144 Å too large, respectively. For the bond angles, significant disparities in BLYP and BP86 for $\theta_{F-C-H'}$, $\theta_{F-C-H''}$, and θ_{C-N-H} are observed, all more than 2°: B3LYP is somewhat better with deviations under 1.5°. The only significant torsional deviation is $\tau_{H-N-C-H'}$, for which BLYP and BP86 deviate by 1.4° and 1.6°, respectively.

For the $FCH_3 \cdot NH_2^-$ product ion−molecule complex, again of C_s symmetry, one immediately observes that the amine group has been pushed up above the unique methyl hydrogen. This migration is much more extreme for the density functionals. The DFT methods all have θ_{F-C-N} in the 129−135° range, whereas CCSD(T) has it at only 8° from linearity. As we have seen before, the large deviation between the density functionals and the coupled cluster standard is in a flat region of the potential surface. The energy required to make $\theta_{F-C-N} = 180°$ is only 0.85 kcal mol^{-1} (B3LYP/TZ2Pf+dif level, freezing all other coordinates). The r_{F-C} distance is increased by about 0.04 Å when compared to isolated CH_3F. Just as in $[F-CH_3-NH_2]^{-\ddagger}$, we see large deviation in r_{C-N}. In this case, all of the functionals deviate by over 0.2 Å. This DFT deficiency, in conjunction with the large θ_{F-C-N} disparity is striking. The angle deviations for $\theta_{F-C-H'}$ and $\theta_{F-C-H''}$ are also over 2°. Finally, we find very large deviations for $\tau_{H''-C-F-H'}$, with B3LYP and BP86 both deviating by 10°.

The energetics of this reaction are listed in Table 8. In both the forward and reverse reaction, both coupled cluster methods

TABLE 8: Energetics (kcal mol^{-1}) of the $CH_3NH_2 + F^- \rightarrow CH_3F + NH_2^-$ Reaction[a]

	E^b_{F,NH_2}	E^w_{F,NH_2}	E^*_{F,NH_2}	$E^b_{NH_2,F}$	$E^w_{NH_2,F}$	$E^*_{NH_2,F}$	E^0_{F,NH_2}
				DZP + dif			
B3LYP	34.98	−17.25	52.23	−5.99	−13.00	7.02	40.97
BLYP	29.29	−17.21	46.50	−9.66	−12.89	3.23	38.95
BP86	30.19	−18.36	48.55	−9.23	−13.03	3.80	39.42
CCSD(T)	39.17	−17.37	56.54	−3.61	−13.72	10.11	42.78
				TZ2P + dif			
B3LYP	33.26	−17.03	50.29	−6.55	−11.78	5.23	39.81
BLYP	27.86	−16.81	44.68	−10.36	−11.78	1.42	38.22
BP86	28.54	−18.13	46.67	−9.90	−11.84	1.93	38.44
CCSD(T)	35.59	−17.66	53.25	−5.83	−12.94	7.11	41.42
				TZ2Pf + dif			
B3LYP	33.38(30.65)	−17.06(−17.00)	50.44(47.65)	−5.63(−4.52)	−11.67(−10.86)	6.04(6.34)	39.01(35.17)
BLYP	27.97(24.90)	−16.85(−16.95)	44.82(41.85)	−9.57(−8.80)	−11.63(−11.05)	2.07(2.25)	37.53(33.70)
BP86	28.57(25.58)	−18.20(−18.53)	46.77(44.11)	−9.09(−8.26)	−11.74(−11.12)	2.66(2.86)	37.66(33.84)
CCSD(T)	36.04(33.45)	−18.97(−18.86)	55.01(52.30)	−4.18(−2.99)	−12.85(−12.09)	8.67(9.10)	40.22(36.44)
aug-cc-pVTZ[b]	(31.49)	(−18.27)	(49.76)	(−2.44)	(−11.84)	(9.41)	(33.92)
experiment							35.4

[a] The numbers in parentheses are zero-point corrected. CCSD(T) is zero-point corrected with MP2 frequencies. [b] These are CCSD(T)/aug-cc-pVTZ, frozen-core single points, zero-point corrected with MP2/TZ2Pf+dif frequencies.

are in good agreement for E^w. Note that $|E^w_{F,NH_2}| > |E^w_{NH_2,F}|$, indicating greater stabilization provided by the bond to the amine hydrogen. With respect to the CCSD(T)/aug-cc-pVTZ standard, B3LYP and BLYP are about 1.3 kcal mol^{-1} too small for the forward complexation energies, whereas BP86 is within 0.3 kcal mol^{-1}. For the reverse reaction, all three functionals are with 1 kcal mol^{-1} of the CCSD(T)/aug-cc-pVTZ results. The Shi et al.[27] values are in mixed agreement with ours, $E^w_{F,NH_2} = -5.00$ kcal mol^{-1} being quite poor, and $E^w_{NH_2,F} = -13.78$ kcal mol^{-1} much more adequate. We again find that their MP2/6-311++G** value for the reverse complexation energy is larger than our CCSD(T) values, implying greater stabilization. This is despite their assumed collinear product complex.

The coupled cluster results for the net activation barriers, E^b, are mixed. For the forward reaction the aug-cc-pVTZ value is almost 2 kcal mol^{-1} smaller than the associated TZ2Pf+dif result. For the reverse reaction, the methods agree within 0.6 kcal mol^{-1}. We see huge deviation between the pure functionals and the aug-cc-pVTZ reference, about 6−7 kcal mol^{-1} for both the forward and reverse reaction. In both cases, the pure functionals are computing a smaller barrier. B3LYP is better, roughly 1 kcal mol^{-1} too small for the forward reaction, and 2 kcal mol^{-1} too small for the reverse. The Shi et al.[27] values, $E^b_{F,NH_2} = 40.09$ kcal mol^{-1} and $E^b_{NH_2,F} = -6.13$ kcal mol^{-1}, are quite poor.

For the reaction energy, E^0_{F,NH_2}, the coupled cluster results deviate substantially, with aug-cc-pVTZ calculating a 2.52 kcal mol^{-1} less endothermic reaction. The CCSD(T)/aug-cc-pVTZ result is roughly 1.5 kcal mol^{-1} smaller than the experimental value. B3LYP is in excellent agreement with the experimental value, while the pure functionals better approximate the CCSD(T)/aug-cc-pVTZ calculation. The Shi et al.[27] MP2/6-31++G** value of 46.22 kcal mol^{-1} does not compare favorably with the present CCSD(T) calculations.

In summary, the $CH_3NH_2 + F^-$ reaction has similar characteristics to its methanol and methanethiol counterparts: a backside reactant complex is precluded by a strong frontside adduct involving hydrogen bonding to a single, acidic proton, except now in C_1 symmetry and with a much smaller binding energy of 18 kcal mol^{-1}; and the product complex, of electrostatic type, has a nonlinear heavy atom framework with facile, large amplitude distortions which are problematic for theory. The $CH_3NH_2 + F^-$ forward reaction has by far the highest net activation barrier (31 kcal mol$^-$) of the reactions studied here. Nonetheless, the previously observed trends of DFT performance are exhibited again with remarkable regularity: complexation energies generally reliable to within 2 kcal mol^{-1}; reasonable B3LYP barriers about 2 kcal mol^{-1} too low; and erroneous BLYP and BP86 barriers more than 5 kcal mol^{-1} too small.

H. $CH_3PH_2 + F^- \rightarrow CH_3F + PH_2^-$. The reaction of methylphosphine with fluoride has not been previously studied theoretically, at least to our knowledge. The structures for the stationary points are detailed in Figure 10. Just as in the methylamine case, the first ion−molecule complex has C_1 symmetry, and CCSD(T) optimizations were feasible only with the TZ2P+dif basis. Again, single point CCSD(T)/TZ2Pf+dif energy points were computed at the CCSD(T)/TZ2P+dif optimized geometry. Note a few interesting distinctions for this molecule. Recall that going from $CH_3OH{\cdot}F^-$ to $CH_3SH{\cdot}F^-$ engenders larger charge transfer, and a smaller r_{H-F}. A similar trend manifests itself here. A Mulliken analysis calculates the CH_3PH charge to be −0.82. Now r_{H-F} is only 1.004 Å, just 0.1 Å longer than in isolated HF, whereas r_{P-H_1} is 2.012 Å, 0.6 Å longer than in isolated CH_3PH_2. As in the methylamine case, the major deviations in r_{X-H} are r_{H_1-F} and r_{P-H_1}. B3LYP is best for these, deviating by 0.022 and 0.015 Å, respectively, whereas BLYP and BP86 both deviate by more than 0.06 Å for both bonds. BLYP has the largest deviation for r_{P-C}, namely 0.011 Å. The two bond angles with the largest deviations are θ_{C-P-H_1} and $\theta_{H_2-P-H_1}$. B3LYP has the largest deviation for θ_{C-P-H_1}, 1.6°, whereas BP86 is the worst for $\theta_{H_2-P-H_1}$, deviating by 2.3°. The two torsional angles with very large deviation are τ_{C-P-H_1-F} and $\tau_{H_2-P-H_1-F}$. For both of these torsional angles, the deviations are 3−4° for BLYP, 4.5−5.5° for B3LYP and over 7° for BP86.

The $[F-CH_3-PH_2]^{-\ddagger}$ col, in C_s symmetry, has phosphorus very slightly pushed down toward the mirrored methyl hydrogens, with $\theta(F-C-P) = 179.9$ °. The methyl hydrogens are slightly pyramidalized toward the phosphine group. The r_{P-C} deviations are particularly large, over 0.13 Å for BLYP. The r_{F-C} deviations are smaller, with BLYP having the largest at 0.069 Å. The only angle deviation over 1° is B3LYP for θ_{C-P-H}.

The $FCH_3{\cdot}PH_2^-$ ion−molecule complex, in C_s symmetry, has the phosphine group pushed toward the unique methyl hydrogen. Unlike the amine case, we find the density functionals agreeing

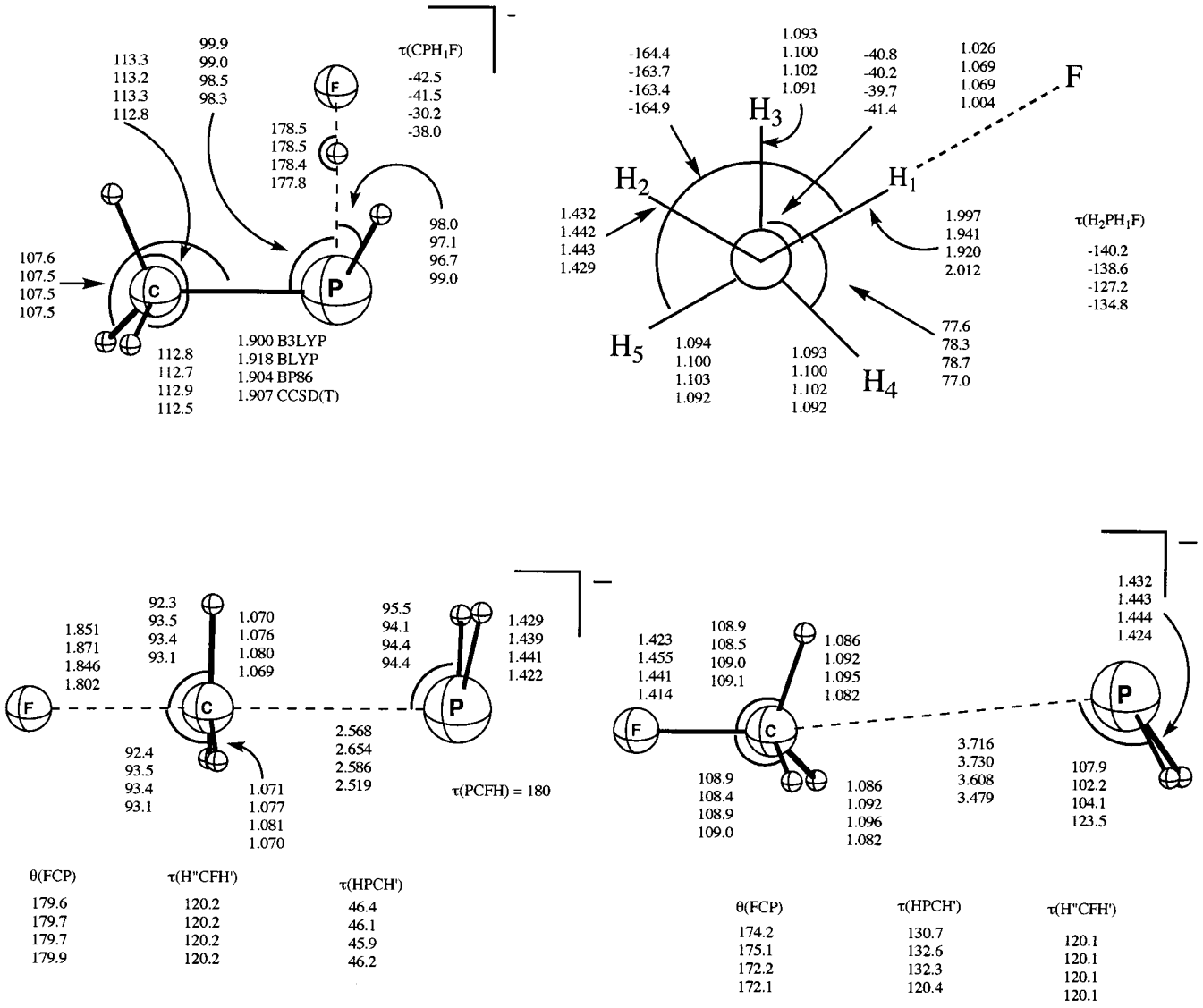

Figure 10. Geometries of the ion−molecule complexes and transition state for the reaction $CH_3PH_2 + F^-$ using the TZ2Pf+dif basis set. All bond distances are in Å, bond and torsional angles in degrees. The top structure is of C_1 symmetry, whereas the bottom two are of C_s symmetry. A Newmann diagram is provided to clarify orientations in the C_1 molecule. For (H′, H″) definitions, see caption to Figure 3. The CCSD(T) values for C_1 ion-molecule complex use the TZ2P+dif basis set.

with the CCSD(T) standard for θ_{F-C-P}. The F−C bond distance is elongated by about 0.03−0.04 Å compared to isolated CH_3F. We find very large r_{C-P} deviations, all over 0.12 Å. BLYP is the worst, 0.251 Å too large. The deviation in θ_{C-P-H} is very large for all the functionals, with BLYP being the worst, at over 21° too small. There is also large deviation in the $\tau_{H-P-C-H'}$ torsional angle, over 10° for all of the functionals.

We now consider the energetics of this reaction, listed in Table 9. Of immediate significance is the disparity between aug-cc-pVTZ and TZ2Pf+dif CCSD(T) values for E^w_{F,PH_2}. The aug-cc-pVTZ complexation energy is over 2 kcal mol^{-1} larger than the TZ2Pf+dif value. The complexation energy for the reverse reaction, $E^w_{PH_2,F}$, finds both basis sets in good agreement. The density functional deviation for E^w_{F,PH_2} is the largest of any complexation energy. B3LYP is over 2.8 kcal mol^{-1} too small. Fortuitously, BP86 is within 0.7 kcal mol^{-1} of the CCSD(T)/aug-cc-pVTZ result. All three functionals are 1.0−1.2 kcal mol^{-1} too small for $E^w_{PH_2,F}$.

The results for the net activation barriers are intriguing. The two coupled cluster values lack agreement. Compared to CCSD(T)/aug-cc-pVTZ, the CCSD(T)/TZ2Pf+dif method computes a barrier 3.19 kcal mol^{-1} too large for the forward reaction, and 1.54 kcal mol^{-1} too small for the reverse. Again, the pure functionals perform abysmally, with deviations of 6−7 kcal mol^{-1} for the forward reaction and 7−9 for the reverse. B3LYP does considerably better than the pure functionals, generally better approximating the CCSD(T)/aug-cc-pVTZ results by 5−6 kcal mol^{-1}.

The results for the reaction energy, E^0_{F,PH_2}, are troublesome. The two coupled cluster computations differ by 4.73 kcal mol^{-1}. In this instance, CCSD(T)/TZ2Pf+dif is much closer to the experimental value of 13.6 kcal mol^{-1}. B3LYP and BP86 compute values within 0.8 kcal mol^{-1} of the CCSD(T)/aug-cc-pVTZ result, while BLYP almost averages the aug-cc-pVTZ and TZ2Pf+dif coupled cluster reaction energies. A preliminary extrapolation of E^0_{F,PH_2} can be made by considering the energy of CCSD(T)/aug-cc-pVTZ + MP2/aug-cc-pVQZ − MP2/aug-cc-pVTZ, which yields 11.41 kcal mol^{-1}. This datum reveals the need for a high-level extrapolation to determine E^0_{F,PH_2} definitively, as performed in our companion study in progress.[114]

In summary the $CH_3PH_2 + F^-$ reaction is analogous in topology to the $CH_3NH_2 + F^-$ reaction. Again we have a

TABLE 9: Energetics (kcal mol^{-1}) of the $CH_3PH_2 + F^- \rightarrow CH_3F + PH_2^-$ Reaction[a]

	E^b_{F,PH_2}	E^w_{F,PH_2}	E^*_{F,PH_2}	$E^b_{PH_2,F}$	$E^w_{PH_2,F}$	$E^*_{PH_2,F}$	E^0_{F,PH_2}
			DZP + dif				
B3LYP	19.02	−19.16	38.18	6.61	−7.40	14.01	12.41
BLYP	14.50	−18.44	32.93	0.94	−7.42	8.35	13.56
BP86	13.80	−22.51	36.31	1.75	−7.44	9.20	12.04
CCSD(T)	27.28	−15.86	43.14	9.47	−9.05	18.52	17.81
			TZ2P + dif				
B3LYP	17.53	−19.10	36.63	5.43	−7.00	12.43	12.11
BLYP	13.17	−18.19	31.36	−0.18	−7.09	6.91	13.35
BP86	12.62	−22.21	34.83	0.59	−7.09	7.68	12.03
CCSD(T)	22.58	−19.01	41.58	5.73	−8.71	14.44	16.84
			TZ2Pf + dif				
B3LYP	17.81(16.46)	−19.32(−19.43)	37.13(35.89)	6.48(6.53)	−6.86(−6.34)	13.34(12.87)	11.33(9.93)
BLYP	13.43(11.90)	−18.39(−18.96)	31.82(30.86)	0.75(0.65)	−6.90(−6.41)	7.65(7.06)	12.68(11.25)
BP86	12.77(11.34)	−22.47(−22.90)	35.25(34.24)	1.56(1.50)	−6.90(−6.52)	8.46(8.02)	11.22(9.84)
CCSD(T)	22.86(21.62)	−20.16(−20.23)	43.02(41.85)	7.72(7.76)	−8.68(−8.14)	16.40(15.90)	15.14(13.86)
aug-cc-pVTZ[b]	(18.43)	(−22.28)	(40.72)	(9.30)	(−7.54)	(16.84)	(9.13)
experiment							13.6

[a] The numbers in parentheses are zero-point corrected. CCSD(T) is zero-point corrected with MP2 frequencies. [b] These are CCSD(T)/aug-cc-pVTZ, frozen-core single points, zero-point corrected with MP2/TZ2Pf+dif frequencies.

frontside reactant complex in C_1 symmetry, followed by a quasilinear F−C−P framework in the $[F-CH_3-PH_2]^{-\ddagger}$ transition state, and another quasilinear product complex, dominated by electrostatics. The binding energy of the reactant complex is larger than that of the $CH_3NH_2 + F^-$ reaction, whereas the opposite is true for the reverse reaction. The forward net and intrinsic activation barriers are 10−12 kcal mol^{-1} smaller than those in the $CH_3NH_2 + F^-$ reaction, whereas the reverse barriers are 7−12 kcal mol^{-1} larger. Again, the pure functionals perform miserably for the barriers, whereas the heretofore adequate B3LYP underestimates the forward complexation energy by almost 2 kcal mol^{-1}, and misses the barriers by more than 2.5 kcal mol^{-1}. The energetics show a trend also manifested in the $CH_3SH + F^-$ reaction, namely large deviation between the aug-cc-pVTZ and the TZ2Pf+dif coupled cluster energetics.

IV. Summary

A systematic database (see information for Supporting Information and ref 114) has been generated and analyzed for the performance of sundry theoretical methods for the prototypical S_N2 systems $CH_3X + F^-$ (X = F, Cl, CN, OH, SH, NH_2, PH_2). The database includes energetics, geometric structures, and harmonic vibrational frequencies of salient stationary points obtained from the B3LYP, BLYP, and BP86 variants of density functional theory as well as the conventional RHF, MP2, CCSD, and CCSD(T) electronic structure methods. For the primary data, basis sets of DZP+dif, TZ2P+dif, and TZ2Pf+dif quality have been used, and final single-point energetics have been determined from high quality focal-point analyses with aug-cc-pVTZ and larger basis sets.[114] The forward and reverse S_N2 reactions of the $CH_3X + F^-$ systems display diverse energetics and topological features, with reaction enthalpies ranging in magnitude from 1 to 36 kcal mol^{-1}, ion−molecule complexation energies scattering from 7 to 38 kcal mol^{-1}, and net activation barriers occurring from −13 to +32 kcal mol^{-1}. The $X^-\cdot CH_3F$ (X = F, Cl, CN, OH, SH, NH_2, PH_2) intermediates are backside, electrostatic complexes with heavy-atom frameworks more or less linear, $F^-\cdot CH_3CN$ is a distorted backside adduct exhibiting a hydrogen bond at a single position, and the $CH_3X\cdot F^-$ (X = OH, SH, NH_2, PH_2) reactant complexes are frontside species with a strong, partially covalent bond to an acidic hydrogen.

The focus of the current paper is a comparison of B3LYP, BLYP, and BP86 density functional results to a reliable CCSD(T) standard, given either by the same basis set or a larger one which satisfactorily approaches the one-particle limit. Although complete sets of DZP+dif and TZ2P+dif data are explicitly presented in Supporting Information and partially characterized in Table 1, we restrict our attention here to the assessment of the TZ2Pf+dif B3LYP, BLYP and BP86 results. Some striking deficiencies in the DFT predictions for the stationary points of the S_N2 reactions are observed. First, the pure functionals erroneously give unimpeded collapse from $F^- + CH_3Cl$ to $FCH_3\cdot Cl^-$, without an intervening reactant complex or transition state. Second, the DFT heavy-atom framework angles in the product complexes generally spread, as much as 43°, from the CCSD(T) standard. Finally, the r_{X-Y} distances in the complexes and transition states are given by the DFT variants to be as much as 0.25 Å too long.

A statistical analysis of the structural data is given in Table 10. The overestimation of r_{X-H} distances is highly systematic, with average absolute TZ2Pf+dif DFT and CCSD(T) differences of 0.006 Å (B3LYP), 0.015 Å (BLYP), and 0.023 Å (BP86) for all systems. Only slightly less systematic, but more severe, are the DFT overestimations of r_{X-Y} distances. For first-row systems, the average absolute deviations for B3LYP, BLYP, and BP86 are 0.027, 0.044, and 0.029 Å, whereas for second-row systems they are 0.053, 0.073, and 0.035 Å, in that order. Thus, due to much better performance for second-row species, BP86 is favored for the critical X−Y distances along the S_N2 reaction paths. The bond angle and torsional angle DFT vs CCSD(T) deviations are not systematic. Due to large disparities for a few complexes, the mean differences are in the 2° range. With only limited preference, the DFT ordering in accuracy is B3LYP > BLYP > BP86. Considering qualitative topology, and both maximum and average errors, B3LYP is the only one of the DFT variants which may be considered to give adequate (but certainly not definitive) geometric structures for these S_N2 systems.

A statistical characterization of the energetic data is given in Table 11. All three DFT schemes appear to underestimate the ion−molecule complexation energies, with mean CCSD(T) differences between 1 and 2 kcal mol^{-1}. BP86 is least favored, having the largest maximum disparity (4−5 kcal mol^{-1}) and the greatest scatter about CCSD(T). In contrast, B3LYP is most favored, exhibiting maximum errors below 3 kcal mol^{-1}, mean differences just over 1 kcal mol^{-1}, and about 90% systematization of the overestimation. For overall reaction energies, the TZ2Pf+dif DFT values for E^0 are systematically smaller than

TABLE 10: Average Absolute Geometric Deviations for Subgroups of S_N2 Reaction Data[a]

	B3LYP	BLYP	BP86
	intermediates and transition states[b]		
r_{total}	0.022(82, 0.244)	0.035(93, 0.251)	0.031(87, 0.205)
r_{X-H}	0.006(89, 0.046)	0.016(92, 0.071)	0.026(91, 0.189)
r_{X-Y}	0.045(73, 0.244)	0.064(94, 0.251)	0.038(82, 0.205)
θ	2.0(53, 39.1)	2.6(50, 37.1)	2.6(58, 42.6)
τ	2.6(44, 11.3)	2.6(40, 14.3)	3.4(52, 15.5)
	first row systems[c]		
r_{total}	0.015(74, 0.244)	0.026(94, 0.246)	0.027(86, 0.205)
r_{X-H}	0.006(87, 0.046)	0.014(95, 0.052)	0.025(92, 0.189)
r_{X-Y}	0.027(56, 0.244)	0.044(93, 0.246)	0.029(78, 0.205)
θ	1.8(67, 39.1)	2.6(46, 37.1)	2.7(69, 42.6)
τ	2.6(50, 11.3)	2.5(50, 14.3)	3.2(50, 15.5)
	second row systems[d]		
r_{total}	0.022(92, 0.237)	0.034(94, 0.251)	0.025(94, 0.130)
r_{X-H}	0.005(97, 0.023)	0.026(91, 0.071)	0.024(94, 0.092)
r_{X-Y}	0.053(84, 0.237)	0.073(100, 0.251)	0.035(93, 0.130)
θ	1.5(46, 15.6)	1.5(46, 21.3)	1.3(46, 19.3)
τ	1.5(60, 10.3)	1.6(47, 12.3)	2.2(67, 11.9)
	all systems[e]		
r_{total}	0.016(82, 0.244)	0.027(94, 0.251)	0.025(89, 0.205)
r_{X-H}	0.006(92, 0.046)	0.015(93, 0.071)	0.023(93, 0.189)
r_{X-Y}	0.034(67, 0.244)	0.049(95, 0.251)	0.029(83, 0.205)
θ	1.7(57, 39.1)	2.1(52, 37.1)	2.1(58, 42.6)
τ	2.1(55, 11.3)	2.1(48, 14.3)	2.7(58, 15.5)

[a] All values pertain to the TZ2Pf+dif basis set. Bond distance deviations are in Å and bond angle and torsional angle deviations are in degrees. Numbers in parentheses are percentage of appropriate coordinates that overestimate the coupled cluster value, followed by the maximum deviation. [b] For all reactions, leaving group anions and neutral substrates excluded. [c] All structures, including reactants and products, for F, CN, OH and NH_2 reactions. [d] All structures, including reactants and products, for Cl, SH and PH_2 reactions. [e] All structures for all reactions.

TABLE 11: Average Absolute Deviations (kcal mol^{-1}) of TZ2Pf+dif DFT Energetic Quantities with Respect to CCSD(T) Standards

	B3LYP	BLYP	BP86
	CCSD(T)/TZ2Pf+dif		
$-E^w$	1.17(85, 2.00)[a]	1.41(92, 2.46)	1.61(67, 4.78)
E^b	2.38(92, 5.16)	6.96(91, 9.72)	6.54(91, 10.28)
E^*	3.24(100, 5.96)	8.13(100, 10.99)	6.43(91, 8.19)
E^0	2.36(83, 4.60)	2.08(83, 2.75)	2.46(83, 4.03)
	CCSD(T)/aug-cc-pVTZ		
$-E^w$	1.29(92, 2.86)	1.47(92, 4.07)	1.17(67, 4.18)
E^b	1.69(92, 2.77)	5.29(100, 8.65)	4.93(100, 7.80)
E^*	2.97(92, 4.83)	7.70(100, 9.87)	6.21(92, 8.82)
E^0	1.26(33, 1.99)	1.72(33, 3.60)	0.80(33, 2.17)

[a] All values are zero-point corrected. All coupled cluster values are zero-point corrected with MP2/TZ2Pf+dif harmonic frequencies. Numbers in parentheses are percentage of appropriate quantities that underestimate the coupled cluster value, followed by the maximum deviation.

their CCSD(T) counterparts, 2−2.5 kcal mol^{-1} on average, but this disparity is reduced to the 0.8−1.8 kcal mol^{-1} range when the comparison is made to aug-cc-pVTZ CCSD(T), which better reproduces the experimental heats of reaction. Finally, the most important result of the assessment of DFT energetics is the documentation of systematic underestimations of the net activation barriers (E^b) for all methods. With respect to the CCSD(T)/TZ2Pf+dif standard, the average absolute E^b errors are 2.38 (B3LYP), 6.96 (BLYP), and 6.54 (BP86) kcal mol^{-1}, and for the more accurate CCSD(T)/aug-cc-pVTZ standard, these disparities are 1.69 (B3LYP), 5.29 (BLYP) and 4.93 (BP86) kcal mol^{-1}. The deficiencies for the intrinsic barriers (E^*) are even more severe. Therefore, only B3LYP can be described as adequate, and the pure functionals clearly fail in predicting the central barriers for these S_N2 reactions.

The inclusion of Hartree−Fock exchange in the density functionals thus appears to be paramount in describing the S_N2 transition states. Indeed, in a very recent paper, Gritsenko and co-workers[115] have shown that the underestimation of the repulsive exchange contribution to the central barrier of the $F^- + CH_3F$ S_N2 reaction is an intrinsic feature of DFT functionals built on the standard generalized gradient approximation (GGA). According to the qualitative rules proposed by these authors, systems exhibiting three center, four electron bonds, with limited nondynamical correlation and delocalized exchange holes, are expected to be spuriously stabilized by GGA functionals, thus leading to anomalously low barriers in the case of S_N2 transition states. Due to the systematic nature of the E^b errors, it is reasonable to speculate that a reparametrization of functionals such as B3LYP to include somewhat more Hartree−Fock exchange would rectify its energetic deficiencies for these pervasive reactions. In an even more recent paper, Lynch and Truhlar[117] discuss the role of Hartree−Fock exchange in the evaluation of barrier heights via density functional theory. They assessed the performance of various hybrid functionals and found that an increase in Hartree−Fock exchange indeed resulted in improved barrier heights (but worse bond and reaction energies). In any event, our data demonstrate a general need for the inclusion of S_N2 complexes and transition states in the molecular parametrization sets for density functionals.

A final point should be highlighted with respect to the $CH_3X \cdot F^-$ ion-molecule complexes for X = OH, SH, NH_2, and PH_2, which are frontside rather than backside adducts. In the chemical reaction dynamics of these S_N2 systems, most of the classical trajectories which lead *directly* from reactants to products are likely to skirt rather than sample the frontside complexes, favoring backside attack instead. However, our work shows that backside ion-molecule *intermediates* do not exist on these potential energy surfaces and that the intrinsic reaction path (IRP) for these displacements does indeed connect the S_N2 transition states to the deep minima of the frontside structures. In these S_N2 cases, the actual potential surfaces do not fit neatly into the classic double-well picture of Figure 1, and it may be fruitful to adopt nonstationary, backside reference structures in the construction of Marcus-theory or other rationalizations of the barrier and reactivity trends. Indeed, the various consequences of the disparity between dynamical and adiabatic S_N2 reaction trajectories warrant further exploration.

Acknowledgment. This research was supported by National Science Foundation Grant No. NSF-CHE9815397.

Supporting Information Available: Tables of geometries in internal coordinates, harmonic vibrational frequencies and absolute energies are available for all structures at the B3LYP, BLYP, BP86, and CCSD(T) levels of theory using DZP+dif, TZ2P+dif, and TZ2Pf+dif basis sets. Additionally, CCSD(T)/aug-cc-pVTZ//CCSD(T)/TZ2Pf+dif absolute energetics are also available. This material is free of charge via the Internet at http://pubs.acs.org.

References and Notes

(1) Brauman, J. I.; Olmstead, W. N.; Lieder, C. A. *J. Am. Chem. Soc.* **1974**, *96*, 4030.

(2) Tanaka, K.; Mackay, G. I.; Payzant, J. D.; Bohme, D. K. *Can. J. Chem.* **1976**, *54*, 1643.

(3) Pross, A.; Shaik. S. S. *New J. Chem.* **1989**, *13*, 427.
(4) DePuy, C. H.; Gronert, S.; Mullin, A.; Bierbaum, V. M. *J. Am. Chem. Soc.* **1990**, *112*, 8650.
(5) Wang, H.; Hase, W. L. *J. Am. Chem. Soc.* **1997**, *119*, 3093.
(6) Uggerud, L. *J. Chem. Soc. Perk. T.* **1999**, *2*, 1459.
(7) Viggiano, A. A.; Midey, A. J. *J. Phys. Chem. A* **2000**, *104*, 6786.
(8) Takeuchi, K.; Takasuka, M.; Shiba, E.; Kinoshita, T.; Okazaki, T.; Abboud, J. L. M.; Notario, R.; Castano, O. *J. Am. Chem. Soc.* **2000**, *122*, 7351.
(9) Davico, G. E.; Bierbaum, V. M. *J. Am. Chem. Soc.* **2000**, *122*, 1740.
(10) Baschky, M. C.; Kass, S. R. *Int. J. Mass. Spectrom.* **2000**, *196*, 411.
(11) Ervin, K. M. *Int. J. Mass Spectrom.* **1998**, *185*, 343.
(12) Su, T.; Wang, H.; Hase, W. L. *J. Phys. Chem. A* **1998**, *102*, 9819.
(13) Tachikawa, H.; Igarishi, M. *Chem. Phys. Lett.* **1999**, *303*, 81.
(14) Li, G.; Hase, W. L. *J. Am. Chem. Soc.* **1999**, *121*, 7124.
(15) Raguei, S.; Cardini, G.; Schetino, V. *J. Chem. Phys.* **1999**, *111*, 10 887.
(16) Tachikawa, H. *J. Phys. Chem. A* **2000**, *104*, 497.
(17) Yamataka, H. *Rev. Heteroatom Chem.* **1999**, *21*, 277.
(18) Okuno, Y. *J. Am. Chem. Soc.* **2000**, *122*, 2925.
(19) Dougherty, R. C.; Roberts, J. D. *Org. Mass. Spectrom.* **1973**, *8*, 81.
(20) Olmstead, W. N.; Brauman, J. I. *J. Am. Chem. Soc.* **1977**, *99*, 4219.
(21) Pellerite, M. J. *J. Am. Chem. Soc.* **1980**, *102*, 5993.
(22) Pellerite, M. J.; Brauman, J. I. *J. Am. Chem. Soc.* **1983**, *105*, 2672.
(23) Dodd, J. A.; Brauman, J. I. *J. Phys. Chem.* **1986**, *90*, 3559.
(24) Lewis, E. S. *J. Phys. Chem.* **1986**, *90*, 3756.
(25) Hoz, S.; Basch, H.; Wolk, J. L.; Hoz, T.; Rozental, E. *J. Am. Chem. Soc.* **1999**, *121*, 7724.
(26) Tonner, D. S.; McMahon, T. B. *J. Am. Chem. Soc.* **2000**, *122*, 8783.
(27) Shi, Z.; Boyd, R. J. *J. Am. Chem. Soc.* **1990**, *112*, 6789.
(28) Bickelhaupt, F. M.; Baerands, E. J.; Nibbering, N. M. M.; Ziegler, T. *J. Am. Chem. Soc.* **1993**, *115*, 9160.
(29) Deng, L.; Branchadell, V.; Ziegler, T. *J. Am. Chem. Soc.* **1994**, *116*, 10 645.
(30) Glukhovtsev, M. N.; Pross, A.; Radom, L. *J. Am. Chem. Soc.* **1994**, *117*, 2024.
(31) Wladkowski, B. D.; Allen, W. D.; Brauman, J. I. *J. Phys. Chem.* **1994**, *98*, 13 532.
(32) Gronert, S.; Merrill, G. N.; Kass, S. R. *J. Org. Chem.* **1995**, *60*, 488.
(33) Glukhovtsev, M. N.; Bach, R. D.; Pross, A.; Radom, L. *Chem. Phys. Lett.* **1996**, *260*, 558.
(34) Botschwina, P.; Horn, M.; Seeger, S.; Oswald, R. *Ber. Bunsen-Ges. Phys. Chem.* **1997**, *101*, 387.
(35) Bickelhaupt, F. M. *J. Comput. Chem.* **1998**, *20*, 114.
(36) Igarishi, M.; Tachikawa, H. *Int. J. Mass Spectrom.* **1998**, *181*, 151.
(37) Aida, M.; Yamataka, H. *J. Mol. Struct. Theochem.* **1999**, *462*, 417.
(38) Mo, Y. R.; Gao, J. L. *J. Comput. Chem.* **2000**, *21*, 1458.
(39) Parthiban, S.; de Oliveira, G.; Martin, J. M. L. *J. Phys. Chem. A* **2001**, *105*, 895.
(40) Kuznetsov, A. M. *J. Phys. Chem. A* **1999**, *103*, 1239.
(41) Craig, S. L.; Brauman, J. I. *J. Am. Chem. Soc.* **1999**, *121*, 6690.
(42) Langer, J.; Matejcik, S.; Illenberger, E. *Phys. Chem. Chem. Phys.* **2000**, *2*, 1001.
(43) Saunders, W. H. *J. Org. Chem.* **2000**, *65*, 681.
(44) Ma, B. Y.; Kumar, S.; Tsai, C. J.; Hu, Z. J.; Nussinov, R. *J. Theor. Biol.* **2000**, *203*, 383.
(45) Jensen, H.; Daasbjerg, K. *J. Chem. Soc. Perk. T.* **2000**, *2*, 1251.
(46) Chabinyc, M. L.; Craig, S. L.; Regan, C. K.; Brauman, J. I. *Science* **1998**, *279*, 1882.
(47) Ayotte, P.; Kim, J.; Kelley, J. A.; Nielsen, S. B.; Johnson, M. A. *J. Am. Chem. Soc.* **1999**, *121*, 6950.
(48) Hase, W. L. *Science* **1994**, *266*, 998.
(49) Farar, J. M. *Annu. Rev. Phys. Chem.* **1995**, *46*, 525.
(50) Wladkowski, B. D.; Lim, K. F.; Allen, W. D.; Brauman, J. I. *J. Am. Chem. Soc.* **1992**, *114*, 9136.
(51) Viggiano, A. A.; Morris, R. A.; Su, T.; Wladkowski, B. D.; Craig, S. L.; Zhong, M.; Brauman, J. I. *J. Am. Chem. Soc.* **1994**, *116*, 2213.
(52) Wang, H.; Hase, W. L. *J. Am. Chem. Soc.* **1995**, *117*, 9347.
(53) Wang, H.; Peslherbe, H.; Hase, W. L. *J. Am. Chem. Soc.* **1994**, *116*, 9644.
(54) Peslherbe, G. H.; Wang, H.; Hase, W. L. *J. Chem. Phys.* **1995**, *102*, 5626.
(55) Peselherbe, G. H.; Wang, H.; Hase, W. L. *J. Am. Chem. Soc.* **1995**, *118*, 2257.
(56) Ryabov, V. M. In *Advances in Classical Trajectory Studies of* S_N2 *Nucleophilic Substitution*; JAI Press: 1993; Vol. 2.
(57) Viggiano, A. A.; Morris, R. A. *J. Phys. Chem.* **1994**, *98*, 3740.
(58) Su, T.; Morris, R. A.; Viggiano, A. A.; Paulson, J. F. *J. Phys. Chem* **1990**, *94*, 8426.
(59) Viggiano, A. A.; Morris, R. A. *J. Phys. Chem.* **1996**, *100*, 19 227.
(60) Viggiano, A. A.; Morris, R. A.; Paschkewitz, J. S.; Paulson, J. F. *J. Am. Chem. Soc.* **1992**, *114*, 10 477.
(61) Hase, W. L.; Cho, Y. J. *J. Chem. Phys.* **1993**, *98*, 8626.
(62) Ziegler, T. *Can. J. Chem.* **1995**, *73*, 743.
(63) Lias, S.; Karpas, Z.; Liebman, J. F. *J. Am. Chem. Soc.* **1985**, *107*, 6089.
(64) Lias, S. G.; Bartmess, J. E.; Liebman, J. F.; Holmes, J. L.; Levin, R. D.; Mallard, W. G. *J. Phys. Chem. Ref. Data 17, supplement 1*, **1988**.
(65) Chase, M. W. Jr. *Technical Report, NIST-JANAF Thermochemical Tables*, 4th ed.; 1998.
(66) Cioslowski, J.; Schimeczek, M.; Liu, G.; Stoyanov, V. *J. Chem. Phys.* **2000**, *113*, 9377.
(67) Hehre, W. J.; Ditchfield, R.; Pople, J. A. *J. Chem. Phys.* **1972**, *56*, 2257.
(68) Francl, M. M.; Pietro, W. J.; Hehre, W. J.; Binkley, J. S.; Gordon, M. S.; Defrees, D. J.; Pople, J. A. *J. Chem. Phys.* **1982**, *77*, 3654.
(69) Becke, A. D. *J. Chem. Phys.* **1993**, *98*, 5648.
(70) Lee, C.; Yang, W.; Parr, R. G. *Phys. Rev. B* **1988**, *37*, 785.
(71) Becke, A. D. *Phys. Rev. A* **1988**, *38*, 3098.
(72) Perdew, J. P. *Phys. Rev. B* **1986**, *33*, 8822.
(73) Čížek, J. *Adv. Chem. Phys.* **1969**, *14*, 35.
(74) Purvis, G. D.; Bartlett, R. J. *J. Chem. Phys.* **1982**, *76*, 1910.
(75) Scuseria, G. E.; Janssen, C. L.; Schaefer, H. F. *J. Chem. Phys.* **1988**, *89*, 7382.
(76) Pople, J. A.; Head-Gordon, M.; Raghavachari, K. *J. Chem. Phys.* **1987**, *87*, 5968.
(77) Huzinaga, S. *J. Chem. Phys.* **1965**, *42*, 1293.
(78) Dunning, T. H. *J. Chem. Phys.* **1970**, *2823*, 53.
(79) Dunning, T. H. *Methods of Electronic Structure Theory*; Plenum Press: 1977; Volume 3, chapter 1, p 1.
(80) Lee, T. J.; Schaefer, H. F. *J. Chem. Phys.* **1985**, *83*, 1784.
(81) Dunning, T. H. *J. Chem. Phys.* **1971**, *55*, 716.
(82) McLean, A. D.; Chandler, G. S. *J. Chem. Phys.* **1980**, *72*, 5639.
(83) Dunning, T. H. *J. Chem. Phys.* **1989**, *90*, 1007.
(84) Kendall, R. A.; Dunning, T. H.; Harrison, R. J. *J. Chem. Phys.* **1992**, *96*, 6796.
(85) Xie, Y.; Grev, R. S.; Gu, J.; Schaefer, H. F.; Schleyer, P. v. R.; Su, J.; Li, X.; Robinson G. H. *J. Am. Chem. Soc.* **1998**, *120*, 3773.
(86) Rienstra-Kiracofe, J. C.; Graham, D. E.; Schaefer, H. F. *Mol. Phys.* **1998**, *94*, 767.
(87) Xie, Y.; Schaefer, H. F.; Fu, X. Y.; Liu, R. Z. *J. Chem. Phys.* **1999**, *111*, 2532.
(88) Brown, S. T.; Rienstra-Kiracofe, J. C.; Schaefer, H. F. *J. Phys. Chem. A* **1999**, *103*, 4065.
(89) Boys, S. F.; Bernardi, F. *Mol. Phys.* **1970**, *19*, 553.
(90) Gutowski, M.; Chalasiński, G. *J. Chem. Phys.* **1993**, *98*, 5540.
(91) Frisch, M. J.; Trucks, G. W.; Schlegel, H. B.; Gill, P. M. W.; Johnson, B. G.; Robb, M. A.; Cheeseman, J. R.; Keith, T.; Petersson, G. A.; Montgomery, J. A.; Raghavachari, K.; Al-Laham, M. A.; Zakrzewski, V. G.; Ortiz, J. V.; Foresman, J. B.; Cioslowski, J.; Stefanov, B. B.; Nanayakkara, A.; Challacombe, M.; Peng, C. Y.; Ayala, P. Y.; Chen, W.; Wong, M. W.; Andres, J. L.; Replogle, E. S.; Gomperts, R.; Martin, R. L.; Fox, D. J.; Binkley, J. S.; Defrees, D. J.; Baker, J.; Stewart, J. P.; Head-Gordon, M.; Gonzalez, C.; Pople, J. A. *Gaussian 94*, revision C.3; Gaussian, Inc.: Pittsburgh, PA, 1995.
(92) ACES II is a program product of the Quantum Theory Project, University of Florida. Authors: Stanton, J. F.; Gauss, J.; Watts, J. D.; Nooijen, M.; Oliphant, N.; Perera, S. A.; Szalay, P. G.; Lauderdale, W. J.; Gwaltney, S. R.; Beck, S.; Balkova, A.; Bernholdt, D. E.; Baeck, K.-K.; Rozyczko, P.; Sekino, H.; Hober, C.; Bartlett, R. J. Integral packages included are VMOL (Almlöf, J.; Taylor, P. R.); VPROPS (Taylor, P.); ABACUS (Helgaker, T.; Jensen, H. J. Aa.; Jorgensen, P.; Olsen, J.; Taylor, P. R.).
(93) Glukhovtsev, M. N.; Pross, A.; Radom, L. *J. Am. Chem. Soc.* **1994**, *118*, 6273.
(94) Schlegel, H. B.; Mislow, K.; Bernardi, F.; Bottini, A. *Theor. Chim. Acta* **1977**, *44*, 245.
(95) Černušák, I.; Urban, M. *Collect. Czech. Chem. Commun.* **53**, *53*, 2239.
(96) Shi, Z.; Boyd, R. J. *J. Am. Chem. Soc.* **1989**, *111*, 1575.
(97) Vetter, R.; Zülicke, L. *J. Am. Chem. Soc.* **1990**, *112*, 5136.
(98) Shi, Z.; Boyd, R. J. *J. Am. Chem. Soc.* **1991**, *113*, 1072.
(99) Shi, Z.; Boyd, R. J. *J. Am. Chem. Soc.* **1991**, *113*, 2434.
(100) East, A. L. L.; Allen, W. D. *J. Chem. Phys.* **1993**, *99*, 4638.
(101) Allen, W. D.; East, A. L. L.; Császár, A. G. In *Structures and Conformations of Non-Rigid Molecules*; Laane, J., Dakkouri, M., van der Vecken, B., Oberhammer, H., Eds.; Kluwer: Dordrecht, 1993; pp 343−373.
(102) Klippenstein, S. J.; East, A. L. L.; Allen, W. D. *J. Chem. Phys.* **1996**, *105*, 118.

(103) Allinger, N. L.; Ferman, J. T.; Allen, W. D.; Schaefer, H. F. *J. Chem. Phys.* **1997**, *106*, 5143.
(104) Császár, A. G.; Allen, W. D.; Schaefer, H. F. *J. Chem. Phys.* **1998**, *108*, 9751.
(105) Wolfe, S.; Mitchell, D. J.; Schlegel, H. B. *J. Am. Chem. Soc.* **1981**, *103*, 7692.
(106) Wolfe, S.; Mitchell, D. J.; Schlegel, H. B. *J. Am. Chem. Soc.* **1981**, *103*, 7694.
(107) Yamabe, S.; Hirao, K. *Chem. Phys. Lett* **1981**, *84*, 598.
(108) Shaik, S. S.; Schlegel, H. B.; Wolfe, S. *J. Chem. Soc., Chem. Commun.* **1988**, *19*, 1988.
(109) Černušák, I.; Diercksen, G. H. F.; Urban, M. *Chem. Phys. Lett.* **1986**, *128*, 538.
(110) Marcos, E. S.; Bertran, J. *J. Chem. Soc., Faraday Trans. 2* **1989**, *85*, 1531.
(111) Riveros, J. M.; Sena, M.; Guedes, G. H.; Xavier, L. A.; Slepetys, R. *Pure and Appl. Chem.* **1998**, *70*, 1969.
(112) Wladkowski, B. D.; East, A. L. L.; Mihalick, J. E.; Allen, W. D.; Brauman, J. I. *J. Chem. Phys.* **1994**, *100*, 2058.
(113) Huber, K. P.; Herzberg, G. *Molecular Spectra and Molecular Structure: Constants of Diatomic Molecules*; Van Nostrand Reinhold Company: 1979.
(114) Gonzales, J. M.; Rocque, B.; Pak, C.; Cox, R. S.; Allen, W. D.; Schaefer, H. F.; Tarczay, G.; Császár, A. G., To be published. Data available at http://zopyros.ccqc.uga.edu/~gonzales/sn2.html.
(115) Gritsenko, O. V.; Ensing, B.; Schipper, P. R. T.; Baerands, E. J. *J. Phys. Chem. A* **2000**, *104*, 8558.
(116) Pitzer, K. S.; Gwinn, W. D. *J. Chem. Phys.* **1942**, *10*, 428.
(117) Lynch, B. J.; Truhlar, D. G. *J. Phys. Chem. A* **2001**, *105*, 2936.